14 Pediatric Imaging

Shereif H. Gamie, Ella Yevdayev, Aarti Kaushik, and Hollie A. Lai

Case 14.1: Adrenal Cortical Cancer

History

A 15-year-old female with known right adrenal cortical adenocarcinoma, status post chemotherapy treatment. PET/CT scan reported pulmonary metastases in the left lung and increase in size in the right adrenal mass.

Findings

Chest: There are two hypermetabolic left lung pulmonary lesions, one in the lateral lingual segment and second at the base (lower lobe), suggesting persistently active pulmonary metastases (measuring approximately 9–10 mm) (Fig. 14.1). The lingular segment nodule, SUV max 4.07. Left lung base nodule, SUV max of 4.07.

Abdomen: A $8.0 \times 4.5 \times 10.8$ cm right adrenal mass, SUV max 18.7 (Fig. 14.2). There are two separate focal areas of intensely increased FDG uptake superior to the mass, more medial, SUV max 18.7 and 12. 7 in the more lateral nodule. Suggestive for metastatic disease. There is noted subtle ill-defined hypoattenuating lesion in the liver seen on unenhanced CT, which demonstrates no significant corresponding FDG uptake on the PET. Lesions seen in the dome of the liver in segment 8 measure approximately 1.2×2.5 cm.

Impression

PET/CT scan demonstrating hypermetabolic pulmonary nodules and right adrenal mass, suggestive for residual metabolically avid local and metastatic disease.

P.S. Conti, A. Kaushik (eds.), *PET-CT*, DOI 10.1007/978-1-4419-5811-2_14

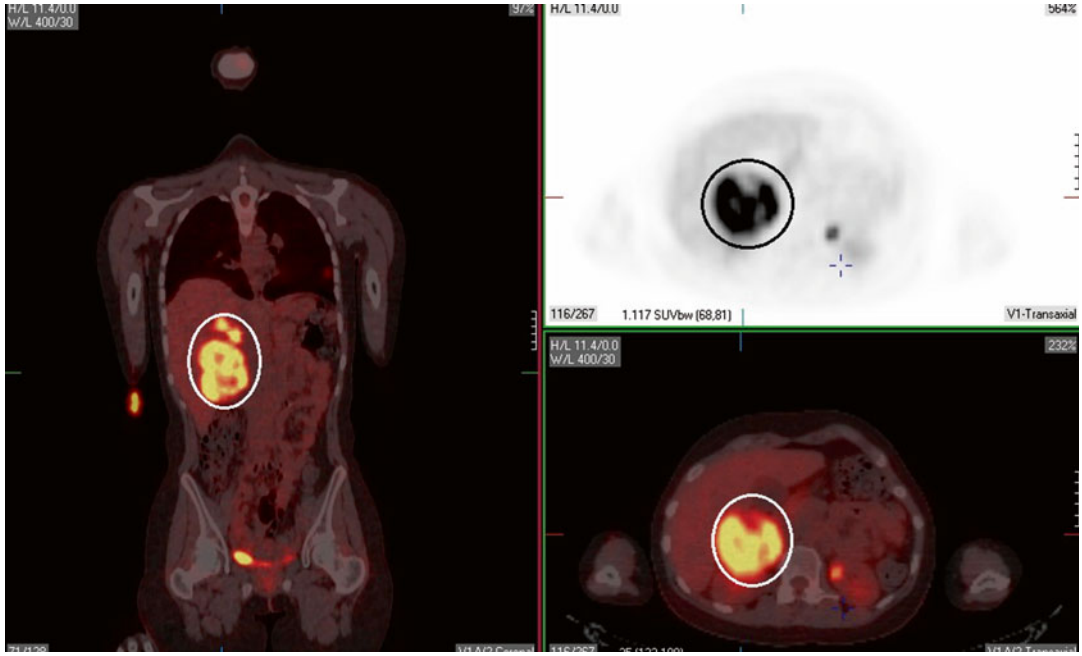

Fig. 14.1

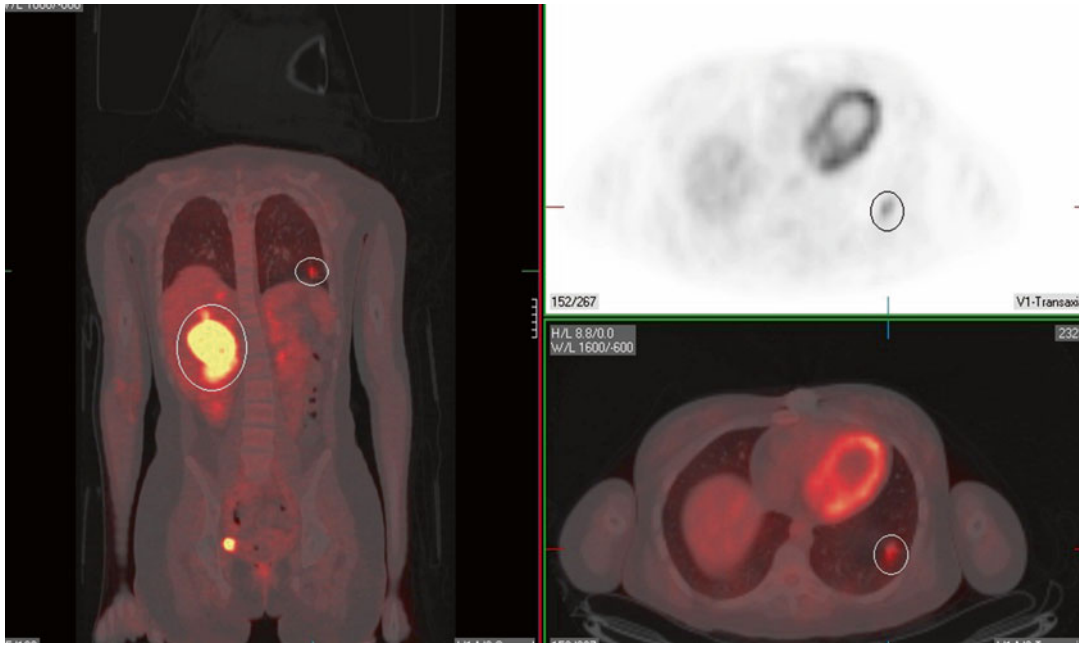

Fig. 14.2

Pearls and Pitfalls

FDG PET for characterization of adrenal lesions showed a sensitivity of 100 %, a specificity of 94 %, and an accuracy of 96 %.

Discussion

Adrenal cortical carcinoma (ACC) is a rare malignant neoplasm with a poor prognosis.

FDG PET showed excellent diagnostic performance in differentiating adrenal lesions detected on CT or MRI. Because FDG PET has the additional advantage of evaluating the primary lesions as well as metastases, it could be cost-effective and the modality of staging. Most adrenocortical carcinomas accumulate and retain FDG and thus can be visualized by PET. However, false-negative findings are possible, especially with very small lesions.

Radical surgery of the primary tumor and of local as well as of distant recurrence is the only effective treatment and requires accurate and early localization of recurrent tumors. All known sites of ACC lesions showed markedly increased FDG uptake (Figs. 14.1 and 14.2).

Case 14.2: Thyroid Cancer: Recurrence

History

A 12-year-old female who was discovered to have a right thyroid lobe nodule on routine physical examination which ultimately turned out to be a T3, N1a, Mx papillary thyroid carcinoma. The patient is status post total thyroidectomy, after which she received 50 mCi of I-131. The patient presented with reportedly elevated thyroglobulin levels. Recent whole-body I-123 scan reported no definitive scintigraphic findings of iodine uptake to suggest a site of locally recurrent and/or metastatic disease.

Findings

Neck: A mildly FDG-avid 4 mm right lower cervical node focus of prominent FDG uptake is seen (SUV max 3.21) (Fig. 14.3). Two or three subtle focal areas of mildly increased FDG uptake are noted in the right lower neck on PET in the midst of the brown fat which appears to correspond to the very subtle subcentimeter-sized nodes on unenhanced CT (Fig. 14.4).

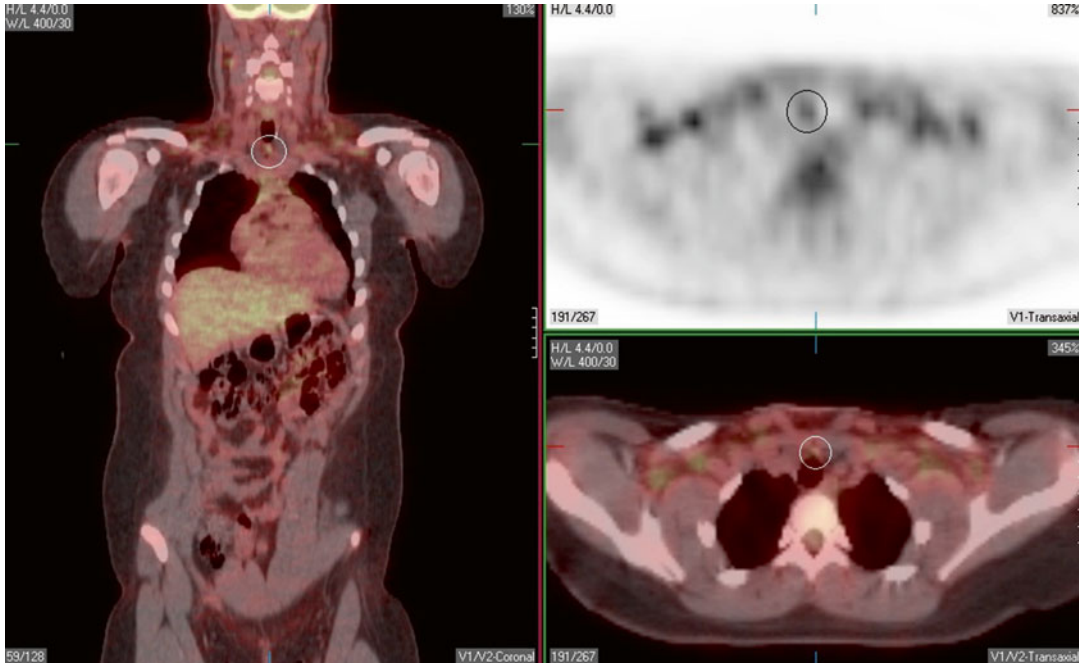

Fig. 14.3

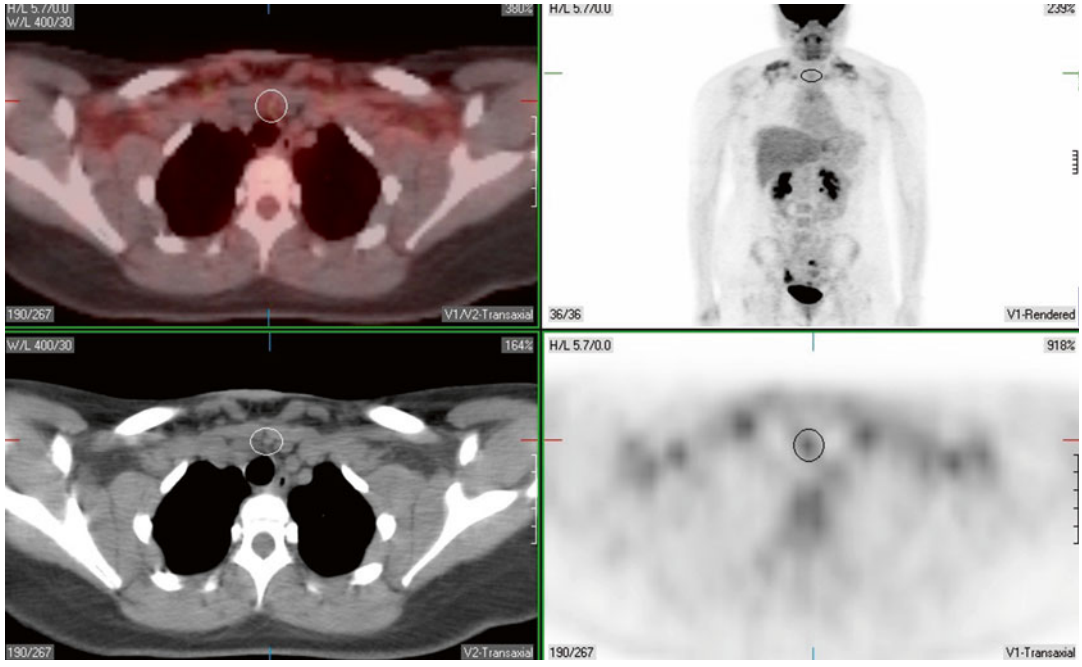

Fig. 14.4

Impression

Restaging PET/CT scan demonstrating subtle subcentimeter-sized mildly FDG-avid nodes in the right lower neck, as detailed above. In the setting of reportedly elevated thyroglobulin levels, these questionable areas of uptake raise concern for possible sites of residual/recurrent disease.

Pearls and Pitfalls

1. Only 50–60 % of papillary thyroid carcinomas and 64–70 % of follicular carcinomas are iodine avid.
2. PET is not indicated for primary thyroid malignancy detection since FDG can accumulate in normal thyroid tissue (about 30 % of patients) and certain benign thyroid disease.
3. A PET study will usually be positive in patients with thyroglobulin level higher than 100 μg/L. PET will detect true positive disease in 11 %, 50 %, and 90 % of patients with hTg levels of <10 μg/L, 10–20 μg/L, and >100 μg/L, respectively.
4. FDG PET/CT is indicated for a known, differentiated, and recurrent papillary/follicular thyroid cancer patients with a negative I-131 scan. Increased expression of GLUT-1 is associated with the loss of radioactive iodine uptake in metastases.

Discussion

Less than 1 % of all cancer death are from thyroid cancer. FNA is best for accurate diagnosis for primary tumor. Coregistered ^{18}F-FDG PET/CT can provide precise anatomic localization of recurrent or metastatic thyroid carcinoma, leading to improved diagnostic accuracy, and can guide therapeutic management. In addition, further assessment of ^{131}I WBS-negative, thyroglobulin-positive patients by ^{18}F-FDG PET/CT may aid in the clinical management of selected cases regardless of the thyroglobulin level (Figs. 14.3 and 14.4).

Case 14.3: Burkitt's Lymphoma

History

A 15-year-old female with reported newly diagnosed Burkitt's lymphoma.

Findings

There are prominent focal symmetric regions of intense FDG uptake bilaterally in the posterior triangle on the upper neck and bilateral supraclavicular regions, which demonstrate no corresponding anatomic correlate on unenhanced CT and likely represent brown fat activity (Fig. 14.5). Tiny, subcentimeter bilateral cervical nodes are seen in the midst of these areas of likely physiologic brown fat activity. There are symmetric regions of intense FDG uptake in the superior mediastinum and bilaterally in the axillae, which demonstrate no corresponding anatomic correlate on CT and also likely represent physiologic brown fat activity (Fig. 14.6). Bilateral symmetric paravertebral intense FDG uptake is seen along the entire thoracic spine, also without corresponding anatomic correlates on CT and also likely physiologic brown fat uptake.

Impression

Prominent most symmetric likely physiologic brown fat activity is seen in bilateral upper neck, supraclavicular regions, superior mediastinum, and axillae. A few scattered subcentimeter nodes are seen in the midst of this brown fat uptake (especially in axillae), in which disease involvement cannot be entirely excluded as detailed above.

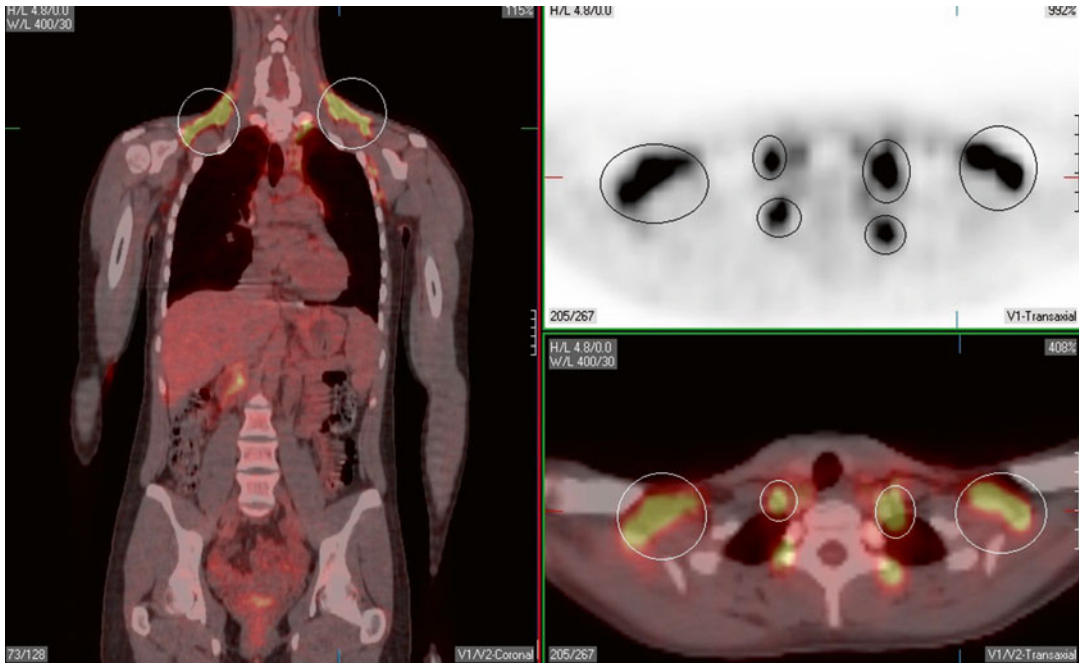

Fig. 14.5

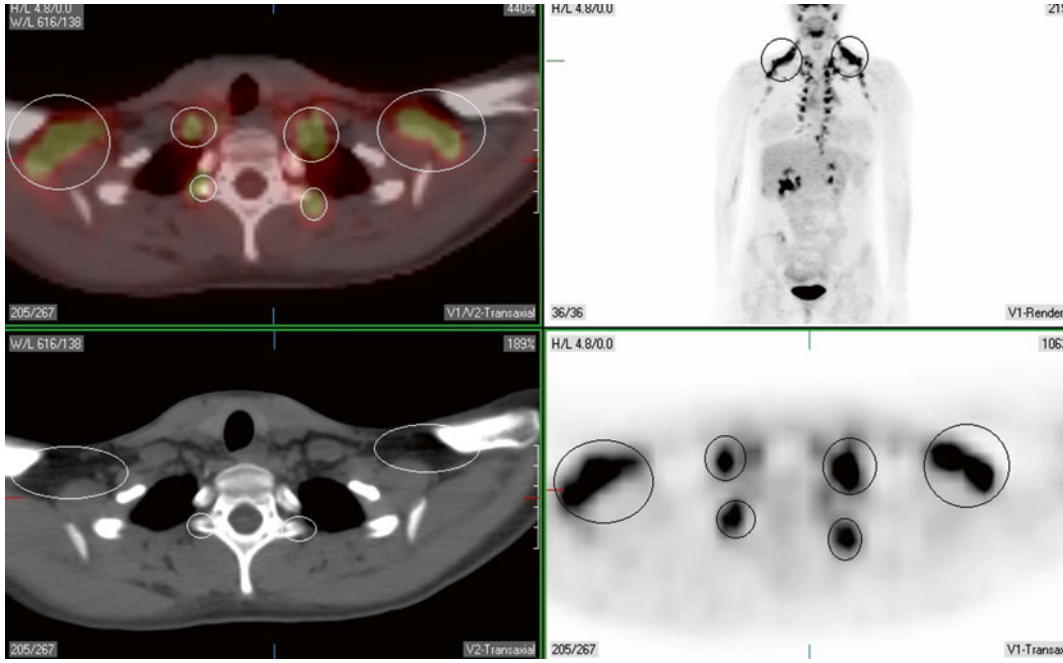

Fig. 14.6

Pearls and Pitfalls

1. Overall sensitivities, specificities, and positive and negative predictive values were 78 %, 98 %, 94 %, and 90 % for F-18 FDG PET and 79 %, 88 %, 90 %, and 46 % for CT, respectively.
2. PET/CT scan with uptake greater than that of the liver is considered positive. Uptake that increased over the background but less than in the liver is equivocal.
3. Coregistered PET/CT images significantly improve the specificity of PET findings. In this case, areas of significant focal FDG uptake in head/neck and chest demonstrate no correlates on CT, enabling differentiation between disease-involved nodes and physiologic brown fat activity.

Discussion

F-18 FDG PET imaging is a useful technique for the staging and follow-up of pediatric patients with lymphoma.

Negative PET/CT scan during routine follow-up for lymphoma in children strongly suggests absence of recurrence, but a positive PET/CT and diagnostic CT scans have low PPV and should be interpreted with caution (Figs. 14.5 and 14.6).

Case 14.4: Hodgkin's Disease

History

A 10-year-old male recently diagnosed with Hodgkin's disease from the left cervical node biopsy and post initiation chemotherapy. Study is performed for scintigraphic staging.

Findings

Head and Neck: Focal region of prominent FDG uptake in seen in the nasopharynx (Waldeyer's ring) more prominent on the left, which corresponds to ill-defined soft tissue fullness on unenhanced CT, which likely represents disease-involved tissue (Fig. 14.7). There is large heterogeneous area of moderate to intense FDG accumulation involving the entire left neck on PET, corresponding to the coalesced-appearing conglomeration of numerous levels II–IV left-sided cervical nodes, which likely represent disease-involved lymphadenopathy. In aggregate, this conglomerate measures approximately 7.5 × 3.6 cm. Several mild to moderate FDG-avid right-sided cervical nodes are seen involving levels II–IV, the largest of these nodes measures approximately 1 × 1.4 cm.

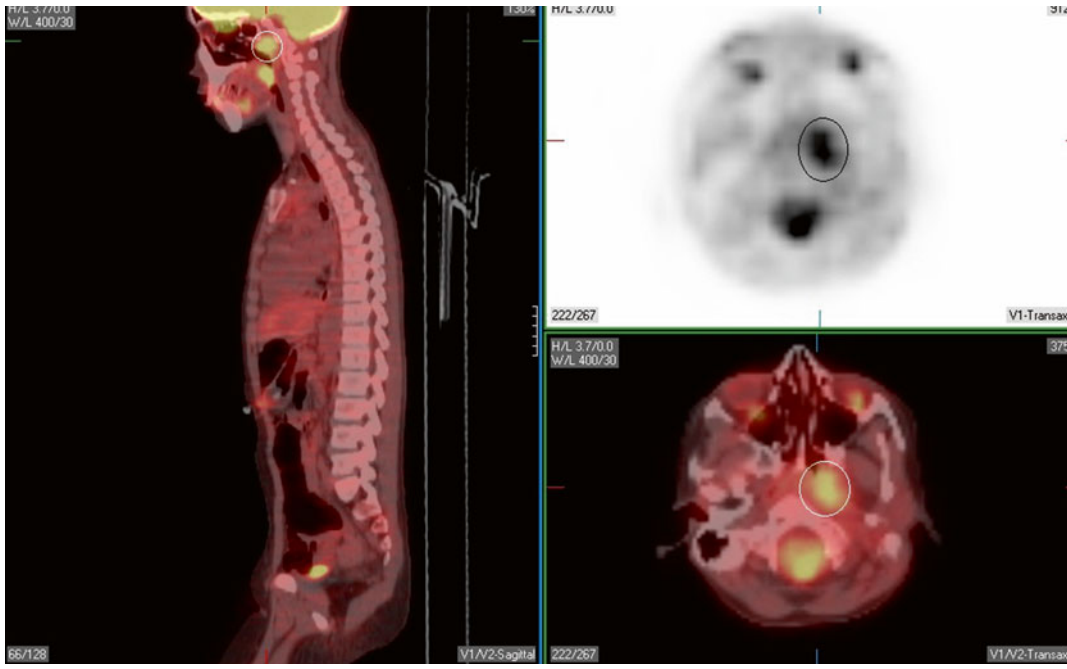

Fig. 14.7

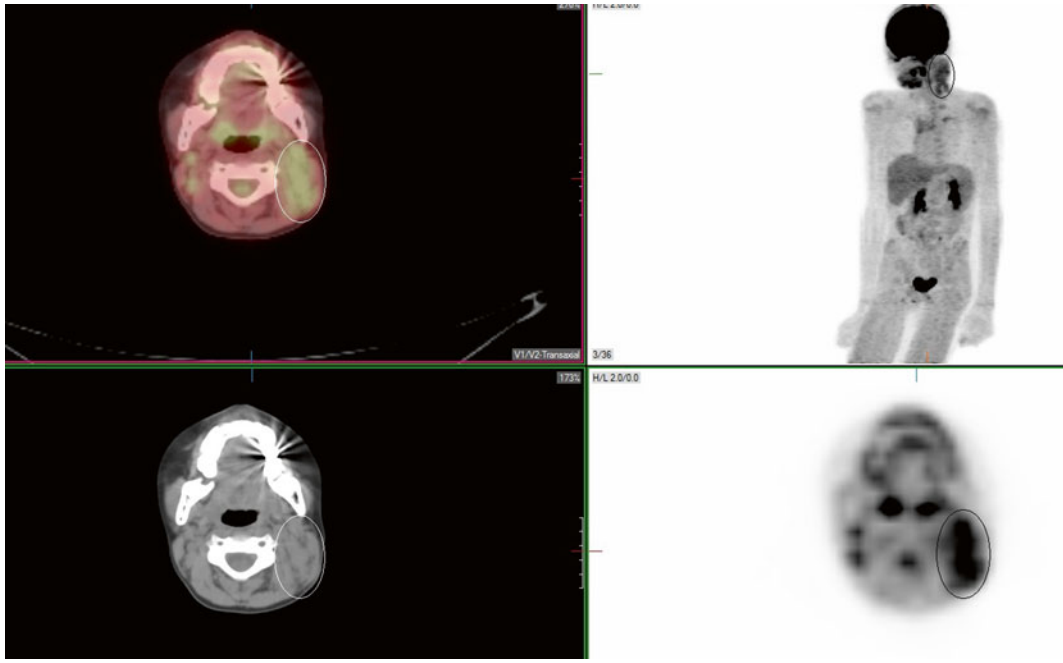

Fig. 14.8

Chest: Diffuse mild curvilinear FDG activity seen in the anterior mediastinum to the left of midline, which may represent reactive/rebound thymic tissue uptake. Left-sided Port-A-Cath seen in the left upper chest.

Abdomen: A focus of intense FDG uptake is seen in the upper anterior abdominal wall, which likely represents reactive uptake in the area of known G-tube (Fig. 14.8).

Impression

PET/CT scan evidence for supradiaphragmatic hypermetabolic lymphadenopathy, predominantly in the Waldeyer's ring and cervical nodes, left more than right, as detailed above.

Pearls and Pitfalls

1. 62–100 % of the FDG-positive patients will relapse after first-line chemotherapy; in contrast, only 4–16 % of the patients with negative PET will relapse.
2. 30–64 % of the residual masses will remain viable following the completion of therapy, demonstrating persistent metabolic uptake.

3. Patient with a negative PET relapse in 16–25 % on a long-term follow-up.
4. 80 % of the patients who relapse do so at another nodal site.

Discussion

The prognosis for children and adolescents with Hodgkin's lymphoma is excellent. However, many patients will show secondary malignancies 15–30 years after the initial diagnosis, which appears to be connected with the intensity of treatment during primary disease. The indication for radiotherapy in patients with early stage Hodgkin's lymphoma should be further refined by using FDG PET for evaluating the response to chemotherapy. Furthermore, in patients at an advanced stage of the disease, it should be determined if sequential FDG PET research during chemotherapy can separate patients into subgroups with an excellent or a poor prognosis.

PET imaging plays an important role in staging, evaluating tumor response, planning radiation treatment fields, and monitoring after completion of therapy for pediatric Hodgkin's lymphoma. This trend will likely increase in the future as a result of PET's superior sensitivity in correlating sites of tumor activity compared to other available functional imaging modalities. Ongoing prospective studies of PET in pediatric patients will increase understanding about the optimal use of this modality in children with cancer and define the characteristics of FDG-avid nonmalignant conditions that may be problematic in the interpretation of tumor activity (Figs. 14.7 and 14.8).

Case 14.5: Rhabdomyosarcoma

History

A 7-month-old infant with reported left thigh rhabdomyosarcoma.

Findings

Chest: Diffuse mild curvilinear FDG activity seen in the anterior mediastinum to the left of midline, which may represent normal physiologic thymic tissue uptake in a 7-month-old infant.

Abdomen: Several moderately to intensely hypermetabolic, likely disease-involved periaortic nodes are seen on PET, the most cranial of which is seen at the level of L3, approximately measuring 0.8 cm (Fig. 14.9).

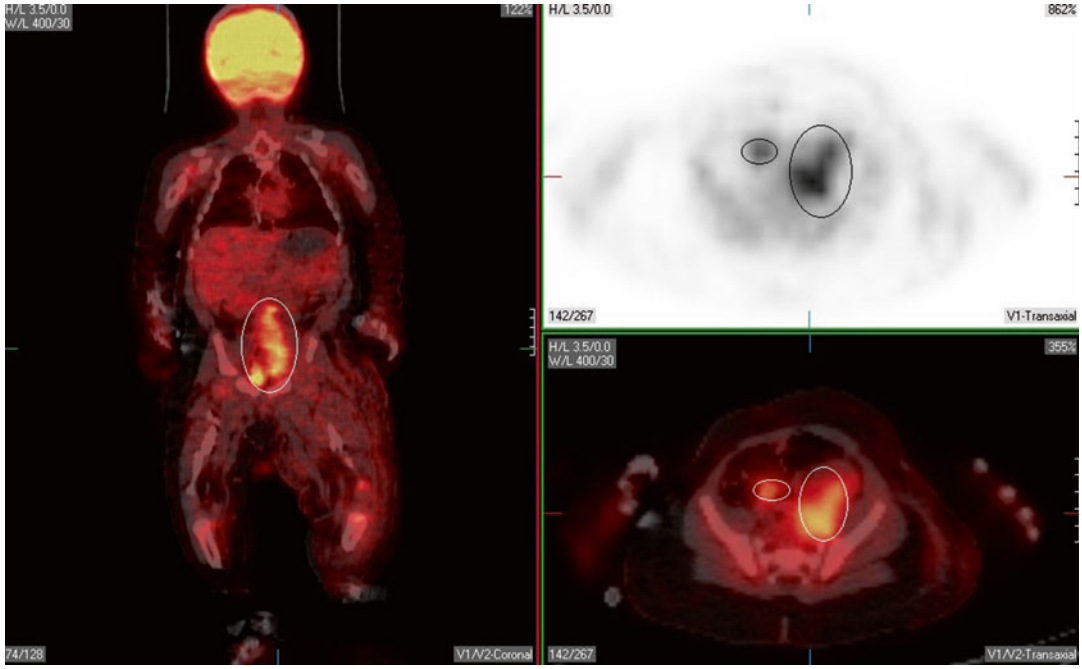

Fig. 14.9

Several adjacent focal regions of moderately intense FDG uptake are seen in the left pelvis/left groin (max SUV 3.69), which corresponds to a cystic appearing confluent mass with a thick periphery in the left pelvis on unenhanced CT, which likely represent bulky left iliac chain necrotic adenopathy, measuring 2.4×1.3 cm.

Several mildly to moderately hypermetabolic left-sided inguinal nodes, the largest of each measures $3 \times 2.1 \times 2.6$ cm on unenhanced CT (Fig. 14.10).

A few scattered mostly subcentimeter right inguinal notes are also seen on unenhanced CT, which demonstrate mild corresponding FDG uptake on PET. Disease involvement cannot be excluded.

Edematous changes are seen in the subcutaneous tissue of the proximal left hip and thigh anteriorly along left thigh edema, likely a mass effect. Undescended right testicle is noted.

Musculoskeletal: Prominent focal region of intensely increased FDG uptake is seen in the posterior and lateral aspect of the left thigh (max SUV 4.87), corresponding to a heterogeneous appearing partially cystic/partially solid bilobed left thigh mass on unenhanced CT, with noted thickened walls and septations (Fig. 14.11). FDG uptake is mostly seen posteriorly in the solid component of this mass, while the more cystic/anterior regions of the mass demonstrate no abnormal FDG uptake.

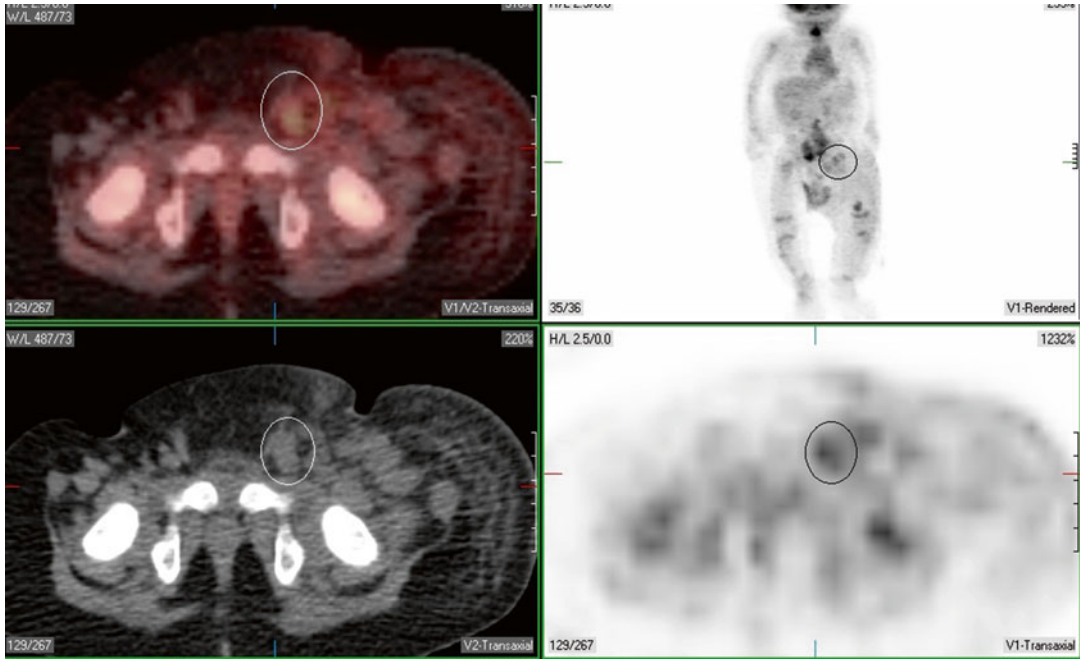

Fig. 14.10

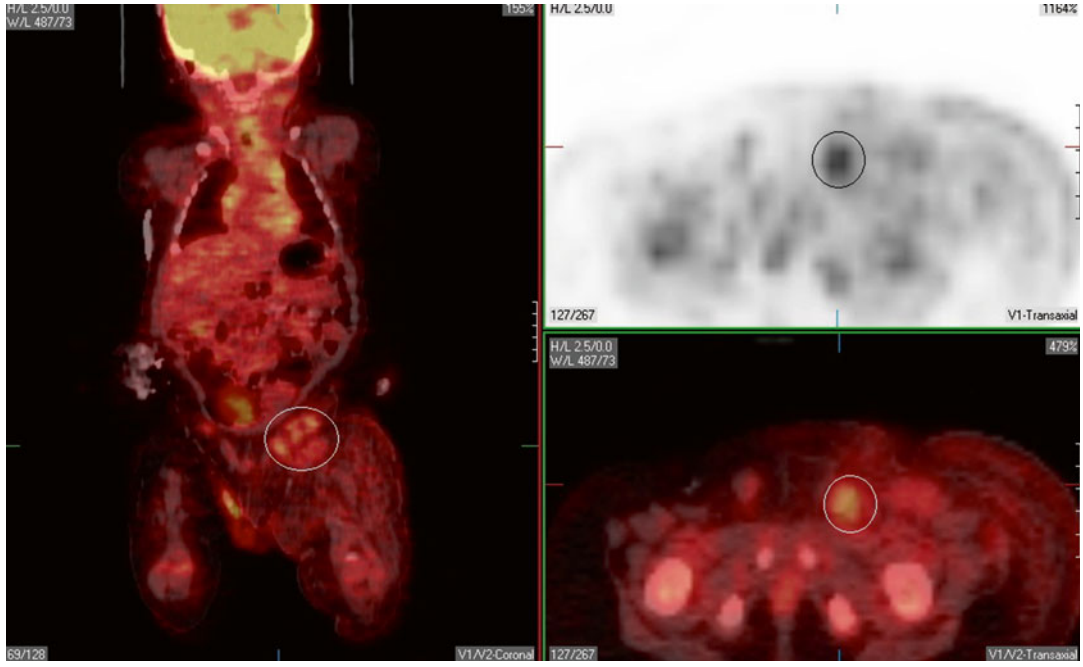

Fig. 14.11

Impression

1. PET/CT scan demonstrates moderately hypermetabolic left thigh mass, which likely represents uptake in the site of the patient's known rhabdomyosarcoma.
2. Moderately to intensely hypermetabolic likely disease-involved periaortic, left iliac, and left inguinal bulky adenopathy, with questionable mildly FDG-avid subcentimeter right-sided inguinal nodes.

Pearls and Pitfalls

1. High-grade sarcomas are generally more FDG-avid than low-grade lesions.
2. Comparing PET with the final clinical determination of disease extent, PET is 77 % sensitive and 95 % specific.

Discussion

PET/CT useful in depicting an unknown primary rhabdomyosarcoma and detecting unsuspected and unusual metastatic sites of childhood sarcomas. It was useful in monitoring response to chemotherapy, radiation therapy, and radiofrequency ablation and aided the postoperative evaluation of tumor resection sites.

^{18}F-fluorodeoxyglucose positron emission tomography (FDG PET) and FDG PET/computed tomography (CT) are becoming increasingly important imaging tools in the noninvasive evaluation and monitoring of children with known or suspected malignant diseases (Figs. 14.9, 14.10, and 14.11).

Case 14.6: Right Kidney Mass and History of Acute Lymphoid Leukemia

History

A 19-year-old female diagnosed with acute lymphoid leukemia as a child who has been in remission since treatment at that time. Recently, the patient reported right abdominal pain, and an abdominal CT reported a 2.8 cm × 2.3 cm × 2.3 cm heterogeneous hyperdense lesion which is partially exophytic in the right lower kidney.

Findings

Abdomen/pelvis: Focal FDG uptake in a 2.8 × 2.3 × 2.3 cm heterogeneous hyperdense lesion in the right lower kidney pole (Fig. 14.12). The SUV max of this lesion is 3.04 on initial whole-body images, and 3.56 on post void delayed spot images of this region (Fig. 14.13). No FDG-avid abdominal and/or pelvic lymph nodes are seen.

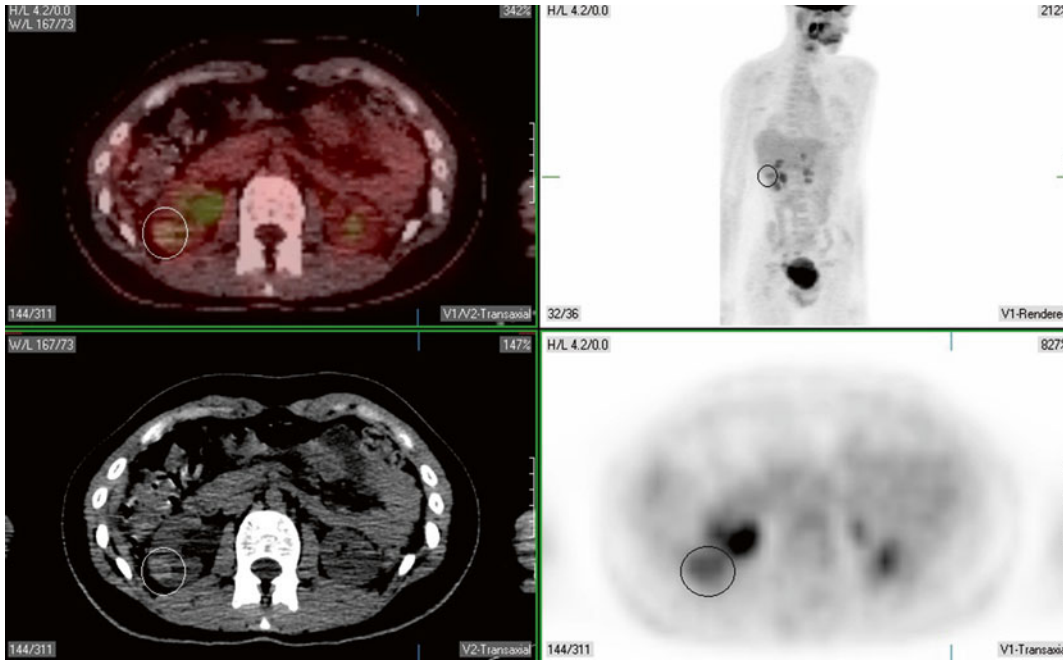

Fig. 14.12

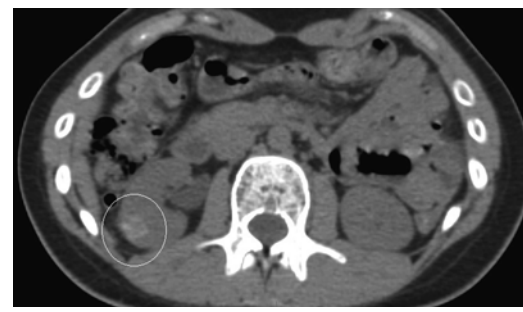

Fig. 14.13

Impression

PET/CT scan demonstrating focal FDG uptake in the right lower kidney pole lesion, which persists on post void/post Lasix augmentation images. Findings raise concern for significant pathology.

Pearls and Pitfalls

FDG PET detected all the sites of distant metastasis revealed by CT, as well as additional metastatic sites, leading to an accuracy of 94 % vs. 89 % for CT. Although PET is more sensitive than CT for the characterization of renal masses, it lacks specificity given a background of physiologic tracer-labeled urine. As such, if we are able to "drive out" all physiologic tracer-labeled urine, we can significantly improve the specificity of PET/CT for these tumors. As such, our now standard acquisition protocol involves injection of 15–20 mg of Lasix IV 25–30 min post FDG administration. Additionally, the acquisition protocol also includes a single post void "bed" of the kidneys, as patient ambulation has proved valuable in allowing gravity to contribute to renal pelvis evacuation.

Additionally, FDG PET has proven to be an efficient tool for the detection of distant metastasis in renal cancer, further suggesting its superiority over CT along. A selection process could be implemented to determine which patients should undergo PET. FDG PET could be performed in the event of a solitary metastasis or doubtful images on CT. Selection could also be based on adverse histological findings from nephrectomy specimens in order to perform staging early after nephrectomy.

Metastatic tumors or secondary lymphoma of the kidney are rare and can often be missed on conventional computed tomography (CT) imaging. On the other hand, many types of metastatic tumor or lymphoma can be detected clearly as hotspots of elevated uptake on FDG PET. However, excreted FDG present in the urinary tract mimics these findings and interferes with image reading. Careful investigation of the renal cortex by FDG PET and review of anatomical images, such as the findings of CT and MRI, have important roles in the detection of renal tumor.

Discussion

F-18 FDG PET may have a role in the diagnostic evaluation of patients with RCC and primary staging of disease. Positive F-18 FDG study may be predictive of the presence of RCC. However, a negative study does not exclude the RCC (Figs. 14.12 and 14.13).

Case 14.7: Chronic Respiratory Disease

History

A 5-year-old male child with reported history of idiopathic interstitial lung disease. The current study is performed to characterize the metabolic nature of areas of most notable inflammatory changes for future comparison to posttreatment scans.

Findings

Chest: The lungs appear hyperexpanded. High-resolution CT of the chest demonstrates diffuse patchy confluent areas of reticular opacities scattered throughout both lungs predominately seen at the lung bases and lower lobes (Fig. 14.14). Corresponding to the confluent reticular opacities is a varying range of mild to moderate intensely hypermetabolic FDG uptake on PET, suggesting metabolic uptake in an area of active inflammatory changes (Fig. 14.15). A region of interest was drawn around the most metabolically active region in the left lung base posteromedially, which demonstrated an SUV max of 1.5 (Fig. 14.16). Another area of curvilinear metabolically increased activity is seen peripherally in the left lower lung lobe with an SUV max of 1.64 (Fig. 14.17). Similarly, the most metabolically active region in the posteromedial right lung base was outlined and showed an SUV max of 1.91 (Fig. 14.18). A focal subcarinal region of

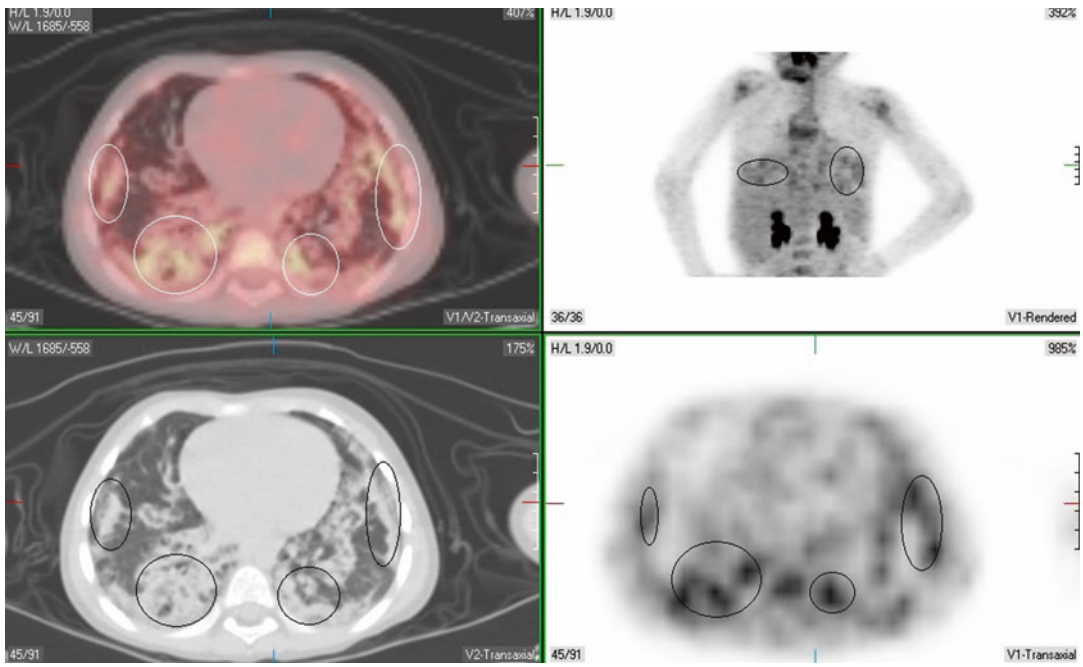

Fig. 14.14

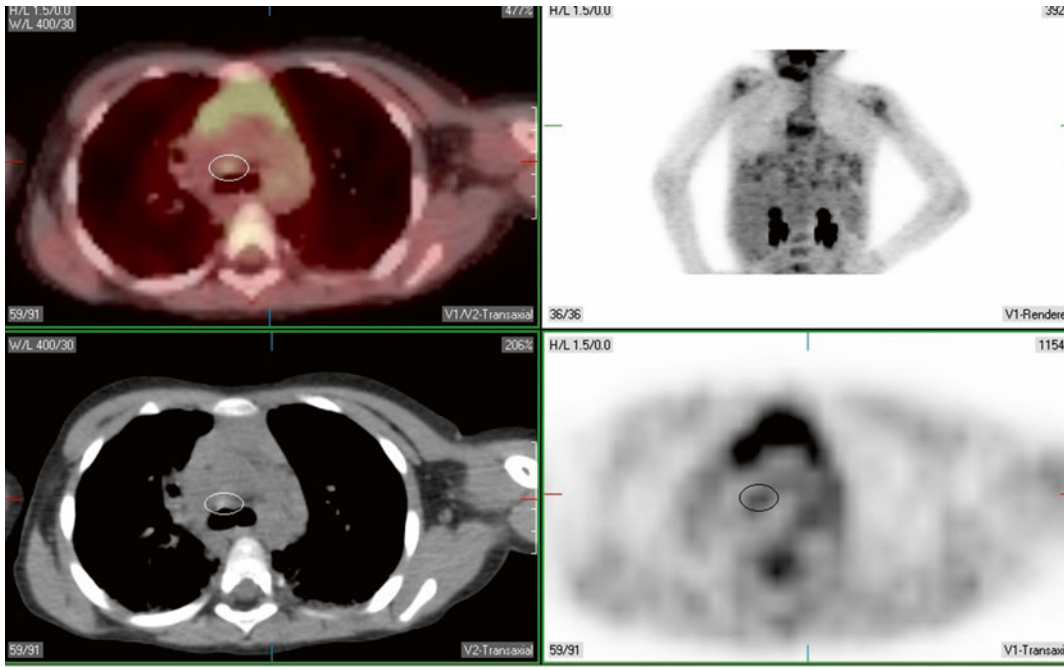

Fig. 14.15

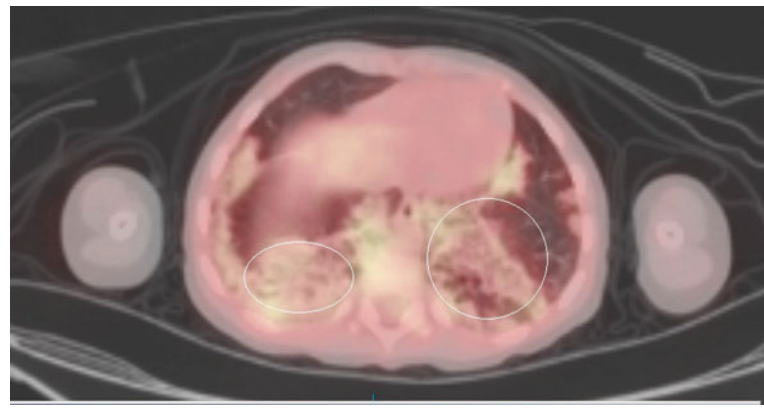

Fig. 14.16

intense FDG uptake is seen with an SUV max of 2.0. Tiny pneumatoceles are seen scattered throughout both lungs along with a few scattered subpleural cysts on unenhanced high-resolution chest CT. A 1.5 cm pneumatoceles is seen at the posterior right lower lung lobe on unenhanced CT, which demonstrates moderately intense FDG uptake on PET. High-resolution images demonstrate mostly parenchymal changes involving bilateral lower lung lobes without peribronchial thickening or bronchiectasis.

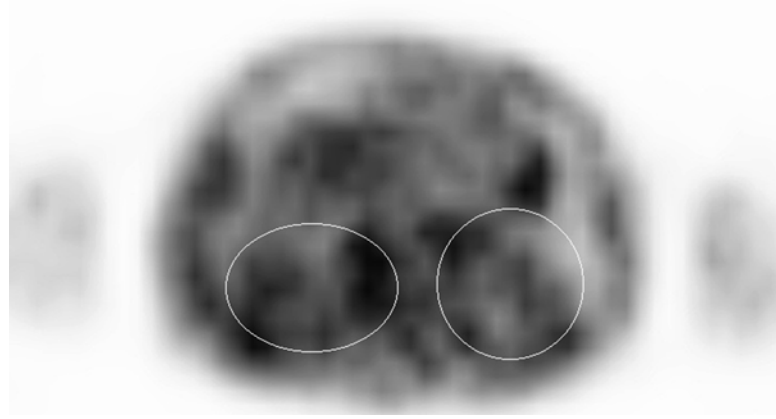

Fig. 14.17

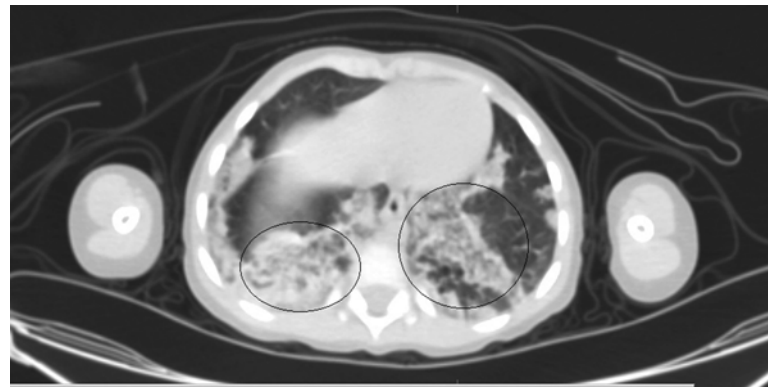

Fig. 14.18

Faint/mild FDG uptake is seen in a 7.0 mm precarinal node. Diffuse nonspecific/similar to background FDG uptake is seen symmetrically in bihilar regions on PET, although evaluation for hilar lymph node enlargement is limited by lack of contrast enhancement. There is no intensely hypermetabolic mediastinal or hilar lymphadenopathy. There are no hypermetabolic axillary lymph nodes. Normal FDG uptake is seen in the heart. Diffuse mild to moderate increased nonspecific likely age-related thymic FDG activity is seen. No pleural or pericardial effusion is seen.

Impression

PET/CT scan demonstrating varying degrees of mild to moderate FDG uptake corresponding to extensive mostly bibasilar lung parenchymal pulmonary opacities with some pneumatoceles and subpleural cysts. SUV max of the most metabolically active regions in both lung bases is as detailed above.

Pearls and Pitfalls

PET does not allow differentiation of IPF from a non-IPF diffuse interstitial pulmonary process.

Discussion

Lung (18)FDG uptake was considered to reflect a gravity-dependent tissue density in the normal lung. Though the lung (18)FDG uptake as well as the CT density tended to be higher in chronic ILD patients, it may be difficult to distinguish them in normal dependent regions from those related to chronic ILD in some cases.

Pulmonary 18F-FDG uptake predicts measurements of health and lung physiology in all patients with IPF and other forms of DPLD. 18F-FDG metabolism is higher when the site of maximal uptake corresponded to areas of reticulation/honeycomb on HRCT than to those with ground-glass patterns (Figs. 14.14, 14.15, 14.16, 14.17, and 14.18).

Case 14.8: Lymphoma

History

A 9-year-old male with recently diagnosed lymphoma. The current study is performed to scintigraphically stage the patient's disease.

Findings

Face/neck: Large bulky conglomerates of hypermetabolic adenopathy are seen involving both sides of the neck which likely represent disease-involved lymphadenopathy (Fig. 14.19).

The largest left neck mass in the posterior triangle measuring approximately $2.3 \times 2.6 \times 2.7$ cm on unenhanced CT, demonstrating an SUV max of 12.1 on PET. Additionally, a separate intensely hypermetabolic nodal mass is seen in the posterior lower left neck/left supraclavicular region measuring 2.3×1.1 cm on unenhanced, with an SUV max of 7.95.

On the right side, the largest nodal mass is seen along the jugular vein measuring $1.5 \times 1.7 \times 2.7$ cm on unenhanced CT demonstrating an SUV max of 10.01 (Fig. 14.20).

Diffuse mild enlargement of the soft tissue of the left posterior pharynx is seen on unenhanced CT with diffuse intensely increased FDG uptake on PET.

Asymmetric tonsillar FDG activity is seen significantly more prominent on the left, corresponding to a more prominent appearing left tonsil in comparison to the right on unenhanced CT. The SUV max on the left tonsil was seen to be 7.98 on PET, measuring 1.4 cm on unenhanced CT.

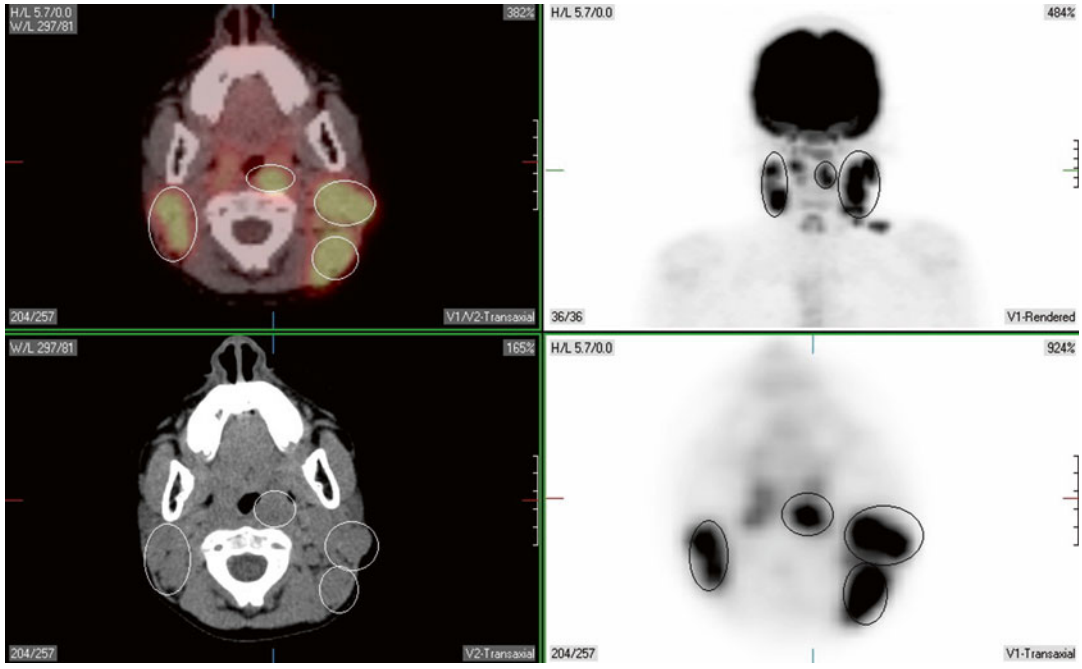

Fig. 14.19

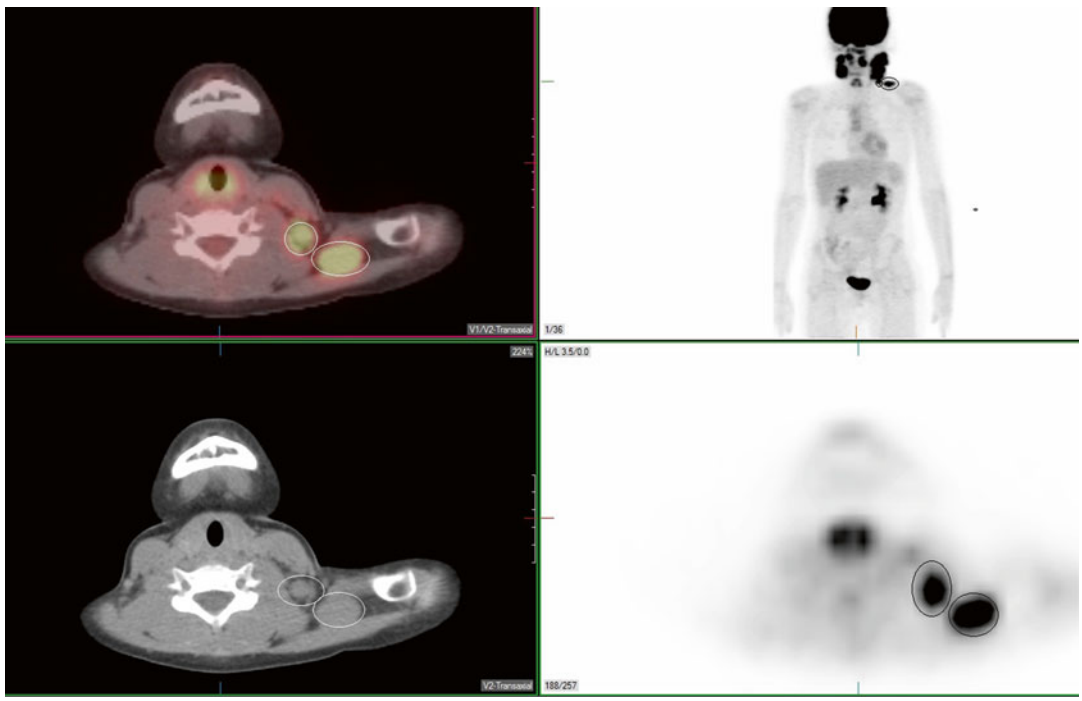

Fig. 14.20

Impression

1. PET/CT scan demonstrating bulky hypermetabolic bilateral cervical and left supraclavicular adenopathy, all of which are likely disease involved.
2. Findings concerning for disease involvement of the posterior pharynx and tonsils (left > right), as detailed above.

Pearls and Pitfalls

1. Overall sensitivities, specificities, and positive and negative predictive values were 78 %, 98 %, 94 %, and 90 % for F-18 FDG PET and 79 %, 88 %, 90 %, and 46 % for CT, respectively.
2. PET/CT scan with uptake greater than that of the liver is considered positive. Uptake that increased over the background but less than in the liver is equivocal.

Discussion

F-18 FDG PET imaging is a useful technique for the staging and follow-up of pediatric patients with lymphoma.

Negative PET/CT scan during routine follow-up for lymphoma in children strongly suggests absence of recurrence, but a positive PET/CT and diagnostic CT scans have low PPV and should be interpreted with caution (Figs. 14.19 and 14.20).

Case 14.9: Leiomyosarcoma

Clinical History

The patient is an 18 -year-old male with a history of metastatic leiomyosarcoma diagnosed in 2007. He has received several rounds of chemotherapy, with the most recent dose in May 2012. The PET scan is requested to evaluate response to therapy.

Findings

Head and Neck: There is a hypermetabolic 1.4 × 0.9 cm left level II lymph node, with a max SUV of 5.2 (Fig. 14.21).

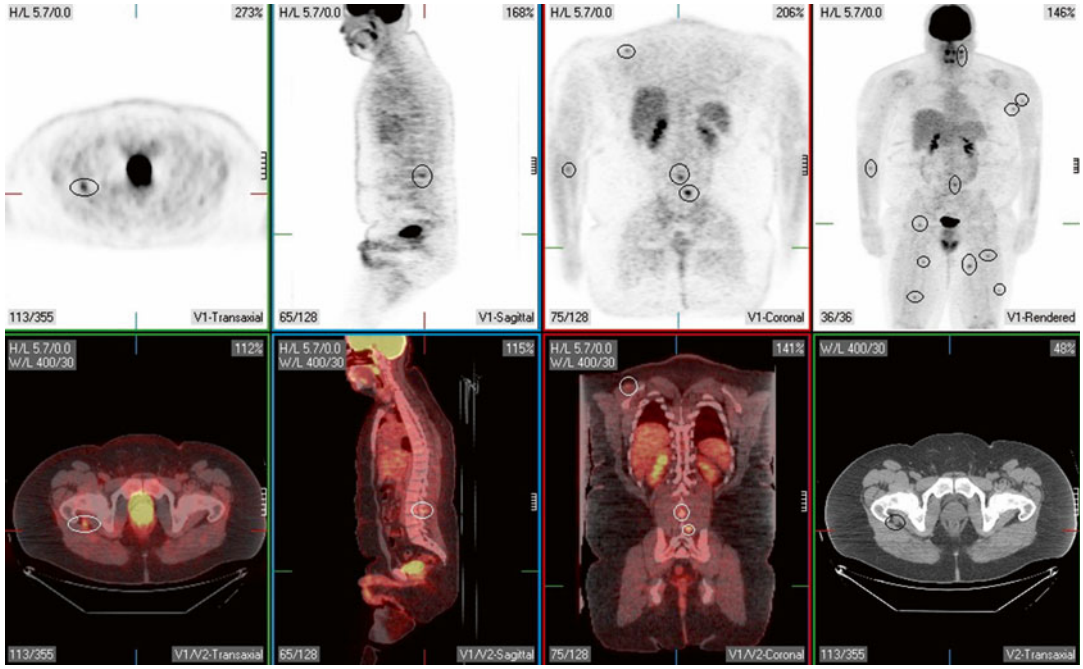

Fig. 14.21

Musculoskeletal System

A small focus in the right upper back posterior to the scapula in or adjacent to the right infraspinatus muscle has a max SUV of 3.5. Two foci are seen in the left upper arm in or adjacent to muscle; this area is suboptimally imaged on CT. Activity in the right upper medial forearm may represent tracer activity at the injection site.

There is a focus of intense activity associated with the paraspinous muscle at the L4 level on the left, max SUV 8.2. A 1×0.7 cm soft tissue density is seen in fat posterior to the right femoral neck, max SUV 5.3. A minimally active 5 mm subcutaneous soft tissue density in the right back at the L1/2 level is of uncertain significance.

Several foci are seen in the lower extremities bilaterally, including in the right upper posterior medial thigh in or adjacent to muscle, max SUV 4.4; a 1×0.6 cm soft tissue density in fat posterior to the right distal femur, max SUV 6.2; a small focus in the right tibialis posterior muscle, max SUV 5.5; a soft tissue density in the left upper anteromedial thigh in fat deep to the sartorius muscle, max SUV 5.1; in the left mid thigh in or closely adjacent to the femur anterolaterally, max SUV 4.7; in the left lateral thigh in muscle; posterior to the left lower femur in or adjacent to muscle; and in muscle in the left medial foot, max SUV 4.0.

Several foci of abnormal activity are seen in bone. The most active (max SUV 8.2) is associated with an approximately 1.2×0.7 cm destructive bone lesion medially in the head of the left mandible. In the right mandible, there is a tiny focus (max SUV 5.3) medially adjacent to the

most posterior molar. Other foci include in the left posterolateral elements of C5 (max SUV 4.9) and in the right side of the spinous process of L3 (max SUV 4.8).

Impression

1. PET/CT imaging demonstrates numerous foci of abnormal tracer uptake in soft tissue of the torso, arms, legs, and left foot and in bone, including in the left and right mandibular heads, the posterolateral elements of c5, the l3 spinous process, and possibly a small focus in the left mid femur.
2. Prominent hypermetabolic left level II lymph node worrisome for malignant involvement.

Pearls and Pitfalls

FDG PET is considered as a useful tool in differentiating a benign lesion from a malignant lesion from benign. However, FDG PET scan was not able to correctly distinguish leiomyosarcoma from benign characteristic of nodular fasciitis. The SUV max in the nodular fasciitis was as high as 7. High glucose uptake in benign lesions was unusual because they normally grow more slowly and are metabolically less active. Why does nodular fasciitis, a benign tumor, has such high FDG uptake? The rapid growth, rich cellularity, and high mitotic activity.

Discussion

FDG PET correctly detected disease in patients with anaplastic thyroid cancer, pleural mesothelioma, myxoid liposarcoma, malignant fibrous histiocytoma, synovial cell sarcoma, and uterine leiomyosarcoma. These findings suggest that PET is useful in the evaluation of a variety of rare tumors both for initial preoperative staging and post-therapy assessment. FDG PET can identify both local and distant recurrences of tumor as a one-step procedure and will detect other metastases (Fig. 14.21).

Case 14.10: Epithelial Malignant Neoplasm

History

The patient is an 18-year-old female with liver cancer (epithelial malignant neoplasm, NOS).

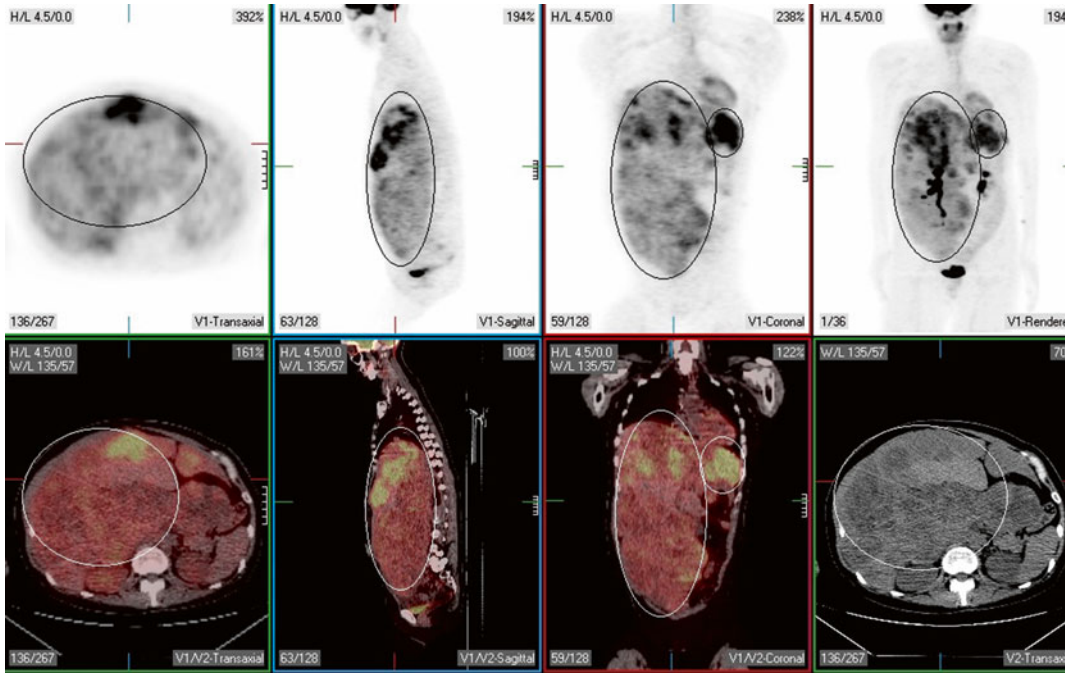

Fig. 14.22

Findings

Abdomen/Pelvis: The liver is studded with numerous hypermetabolic lesions in both lobes corresponding to large confluent hypoattenuating lesions (Fig. 14.22). For reference purposes, the lesion in the anterior right hepatic lobe (segment IV with SUV max of 6.03) and the lesion in the left lateral segment at the same level have an SUV max of 5.0. The spleen measures approximately 9.2 cm.

Impression

PET/CT scan demonstrating numerous large hypermetabolic bilobed hepatic lesions.

Pearls and Pitfalls

1. Data suggests that FDG PET imaging may be able to effectively monitor the efficacy of regional therapy to hepatic metastases. FDG PET is more accurate than lipiodol retention on CT in predicting the presence of residual viable tumor. The presence of residual uptake in some lesions can help in guiding further regional therapy.

2. The sensitivity of FDG PET for detection of HCC is 64 %. A correlation was found between the degree of FDG uptake and the grade of malignancy. Therefore, FDG imaging may have a prognostic significance in the evaluation of patients with HCC. HCCs that accumulate FDG are associated with markedly elevated alpha-fetoprotein levels. However, FDG PET has limited value for the differential diagnosis of focal liver lesions in patients with chronic hepatitis C virus infection because of the low sensitivity for detection of HCC and the high prevalence of this tumor in that population of patients.

Discussion

Ninety percent of malignant primary liver tumors are tumors from epithelial origin: hepatocellular carcinoma (HCC) and cholangiocarcinoma. FDG PET detects only 50–70 % of HCC, but has a sensitivity greater than 90 % for all other primary (cholangiocarcinoma and sarcoma) and metastatic tumors to the liver. FDG PET imaging appears helpful to differentiate malignant from benign hepatic lesions, with the exception of false-negative HCC, false-negative infiltrating cholangiocarcinoma, and false-positive inflammatory lesions. It is not helpful to identify HCC in patients with cirrhosis and regenerating nodules. In patients with hepatic primary malignant tumors trapping FDG, FDG PET imaging does identify unexpected distant metastases (although miliary carcinomatosis is often false negative) and can help in monitoring therapy. Scintigraphic tumor detectability depends on both the size of the lesion and the degree of uptake, as well as surrounding background uptake and intrinsic resolution of the imaging system. Small lesions may yield false-negative results which can be due to partial volume averaging, leading to underestimation of the uptake in small lesions (Fig. 14.22).

Case 14.11: Brown Fat

Findings

Extensive uptake in the neck corresponding to brown fat uptake (Fig. 14.23).

Pearls and Pitfalls

1. Combined ^{18}F FDG PET/CT provides precise anatomic correlation, which allows differentiation between ^{18}F FDG uptake corresponding to fat-attenuation tissue at CT and uptake from pathologic causes.
2. Brown fat ^{18}F FDG uptake can also be avoided by administering diazepam, fentanyl, or propanolol prior to injection.

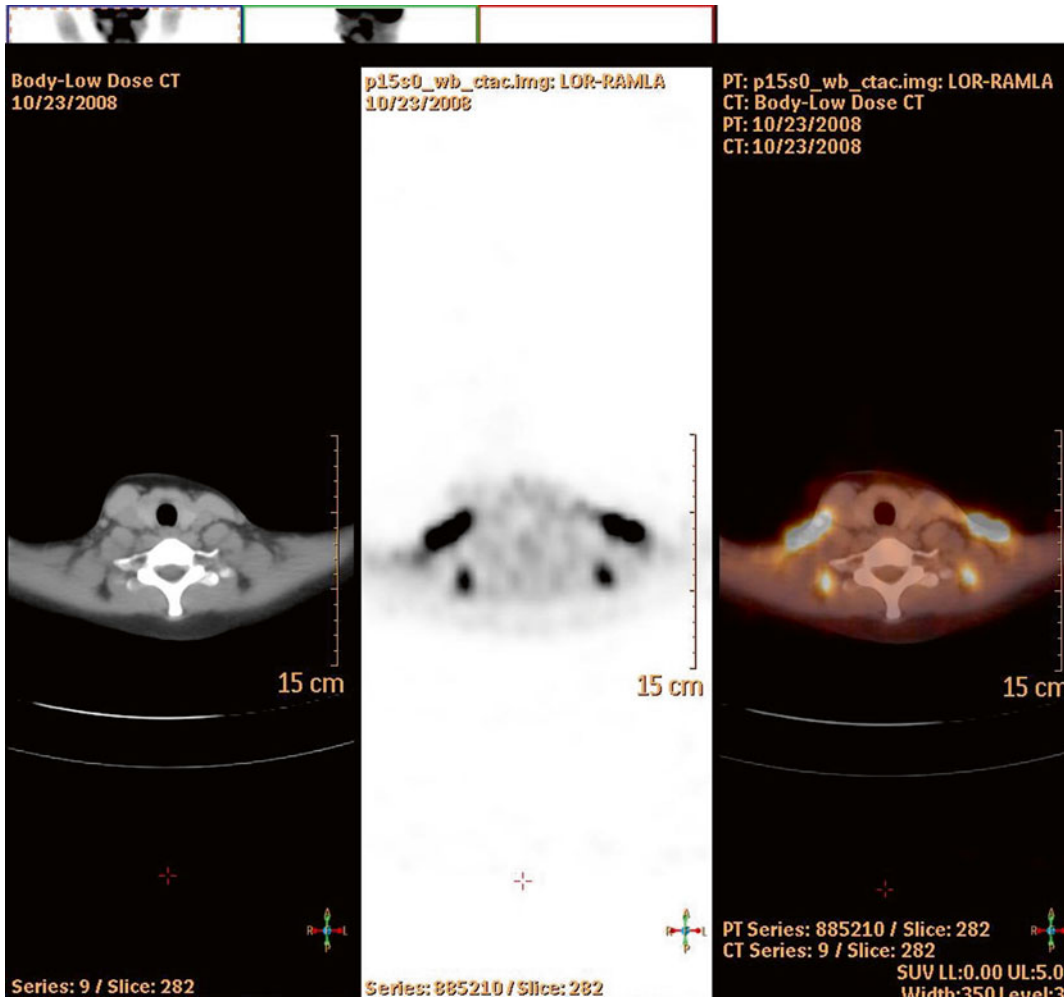

Fig. 14.23

Discussion

The development of PET/CT has led to the recognition that metabolically active fat, referred to as brown fat, can accumulate FDG and represents a possible source of false-positive scans in oncology patients. Physiologic high uptake can be observed along the distribution of activated brown adipose tissue in the neck, supraclavicular regions, axillae, mediastinum, and paravertebral and perinephric regions. Uptake of ^{18}F FDG, a glucose analog, occurs when glucose transporters in brown adipose tissue have been activated. Since the introduction of PET, physiologic ^{18}F FDG uptake in activated brown adipose tissue has been known to be a source of false-positive results. ^{18}F FDG uptake in brown fat is typically bilateral and symmetric. However, focal and asymmetric uptake can occur in the neck or mediastinum, leading to false-positive results. Combined ^{18}F FDG

PET/CT provides precise anatomic correlation, which allows differentiation between ^{18}F FDG uptake corresponding to fat-attenuation tissue at CT and uptake from pathologic causes. Uptake in brown fat is more common in children than in adults and is most common during the winter. Warming the patient prior to injection and during the uptake phase is a simple approach that is used routinely at our institution to reduce brown fat uptake. Brown fat ^{18}F FDG uptake can also be avoided by administering diazepam, fentanyl, or propanolol prior to injection (Fig. 14.23).

Case 14.12: Normal Thymus

Findings

Normal thymic uptake (Fig. 14.24).

Pearls and Pitfalls

Both the higher metabolic activity of the thymus in the first years of life to puberty and the known phenomenon of the occurrence of thymus hyperplasia after chemotherapy were considered.

Discussion

The thymus is a lymphoid organ and endocrine gland responsible for directing and stimulating the adaptive immune system. The thymus gland is located in the superior and anterior mediastinum, behind the sternum. Thymus shape and size demonstrate marked age-related and interindividual variability on ultrasonographic (US), computed tomographic (CT), and magnetic resonance (MR) imaging studies, particularly in early childhood. The thymus is disproportionately large in infants and gradually undergoes involution with fatty replacement by adolescence or early adulthood. The normal thymus is typically triangular or bilobed in shape with homogeneous parenchyma and absence of mass effects on adjacent structures. The thymus responds to systemic stress related to infection, neoplasm, chemotherapy, and surgery by rapid atrophy. Once the stressful event has ended, the thymus may regrow to its original size and beyond. In patients with malignant mediastinal tumors, the thymus typically regresses during chemotherapy, with possible rebound enlargement after completion of therapy (Fig. 14.24).

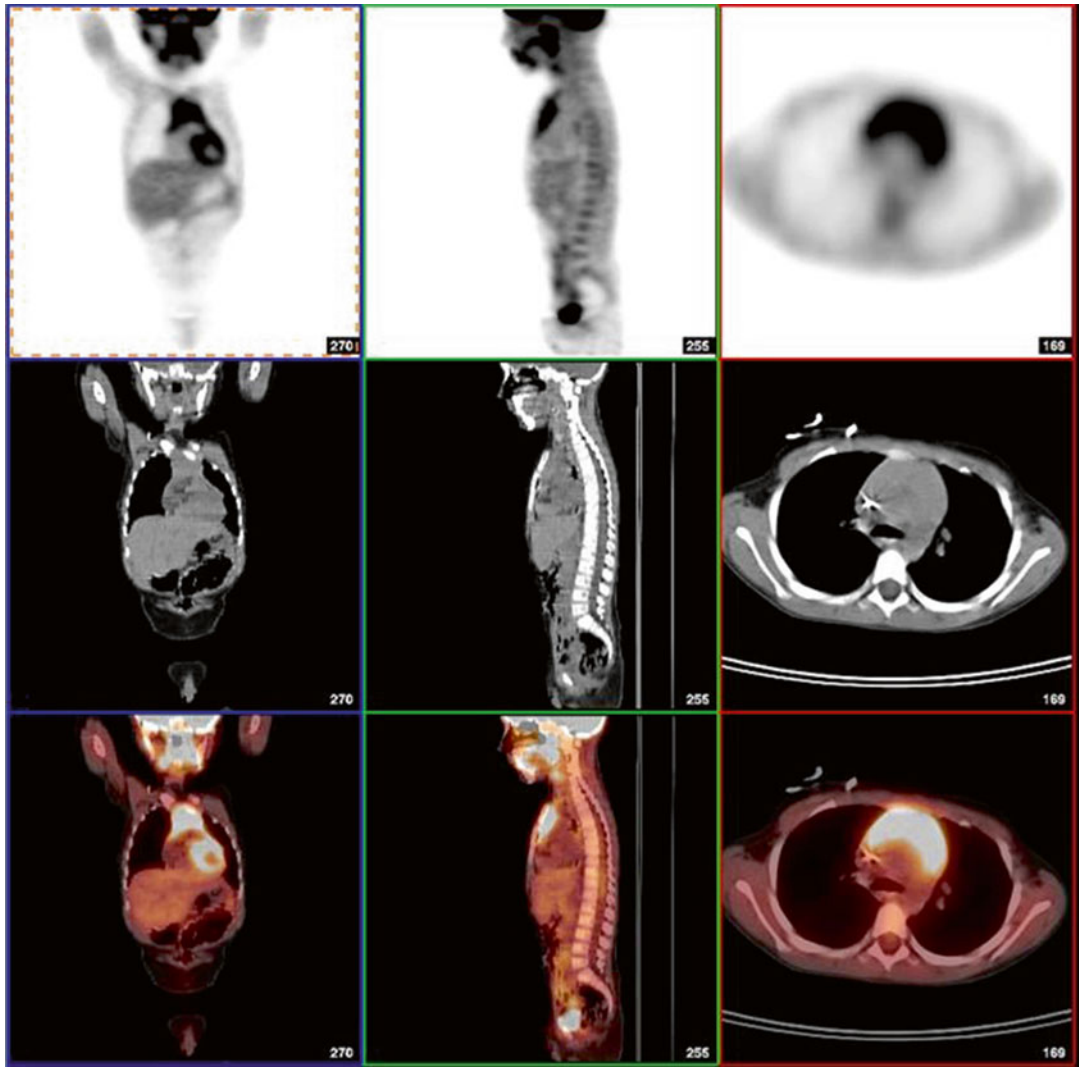

Fig. 14.24

Case 14.13: Pediatric Lymphoma

Findings

Uptake in multiple left lymph nodes (Fig. 14.25). Biopsy was consistent with Hodgkin's lymphoma.

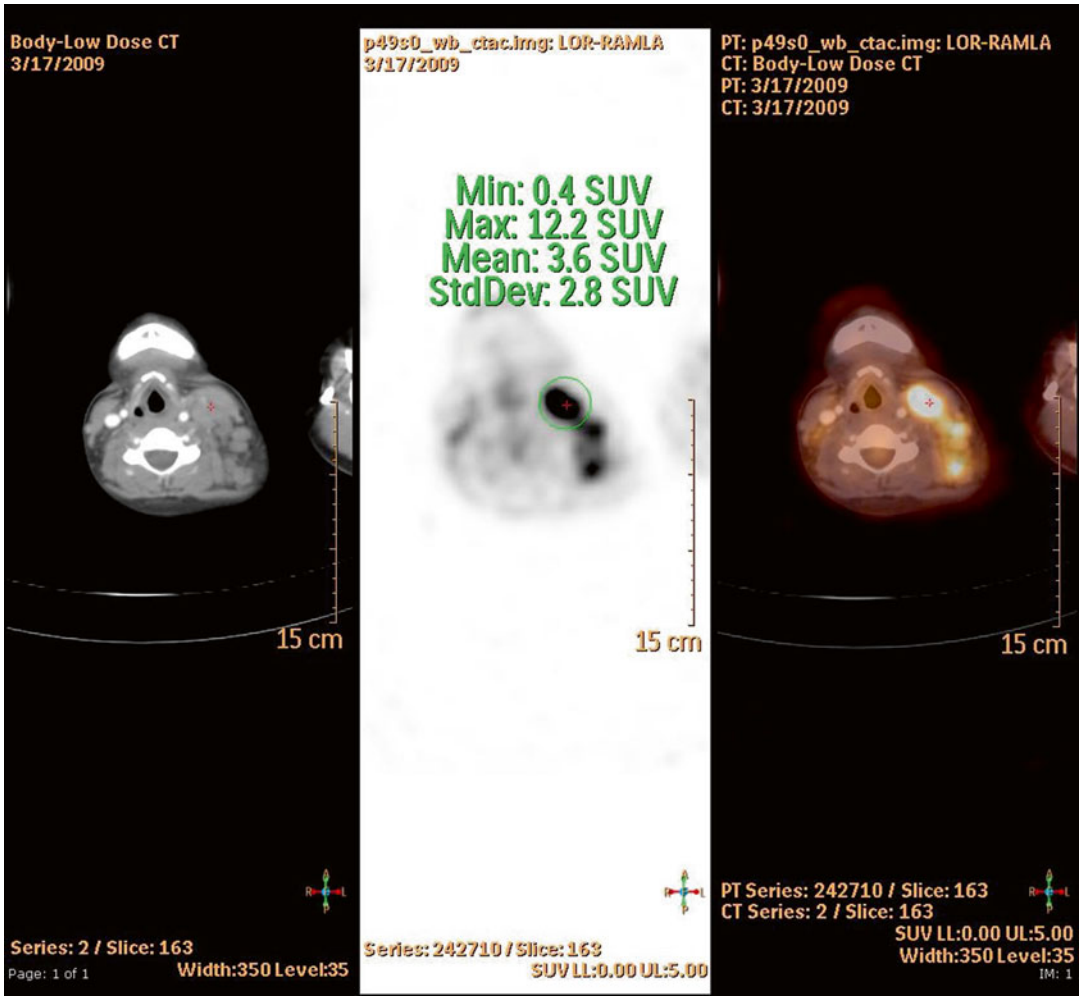

Fig. 14.25

Pearls and Pitfalls

Bone marrow biopsy is the reference standard for BMI; it can miss localized disease outside the site of bone marrow biopsy. FDG PET/CT may be used at initial staging of pediatric lymphoma as it may uncover unsuspected bone marrow involvement.

Discussion

PET/CT in pediatric lymphoma is more accurate than other imaging modalities for initial staging, evaluating treatment response and follow-up (Fig. 14.25).

Case 14.14: NUT Midline Carcinoma

Findings

Uptake in chest corresponds to the patient's primary NUT midline carcinoma (Fig. 14.26). There are also osseous metastases to the humeri, spine, femurs, and tibias (Fig. 14.27).

Discussion

NUT midline carcinoma is a very rare, poorly differentiated, highly aggressive cancer originating from midline body locations, most often in

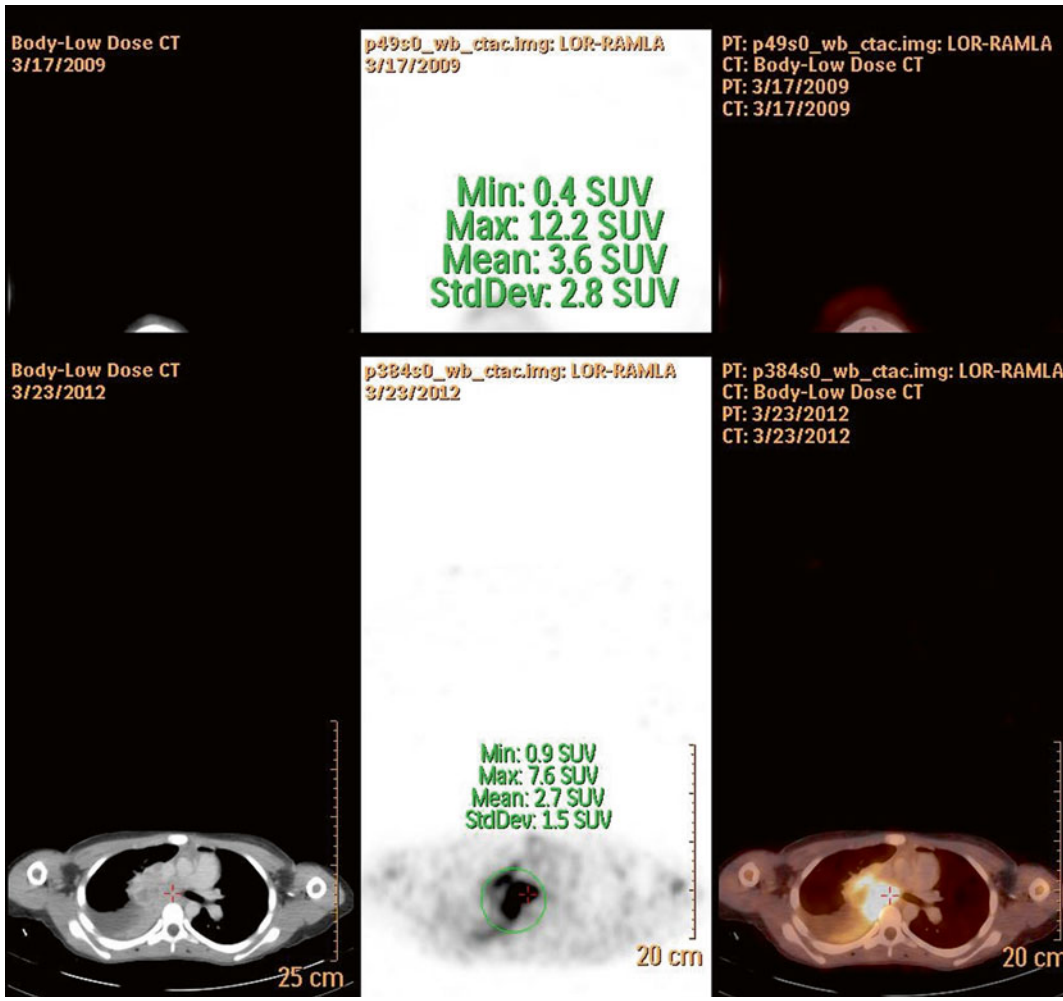

Fig. 14.26

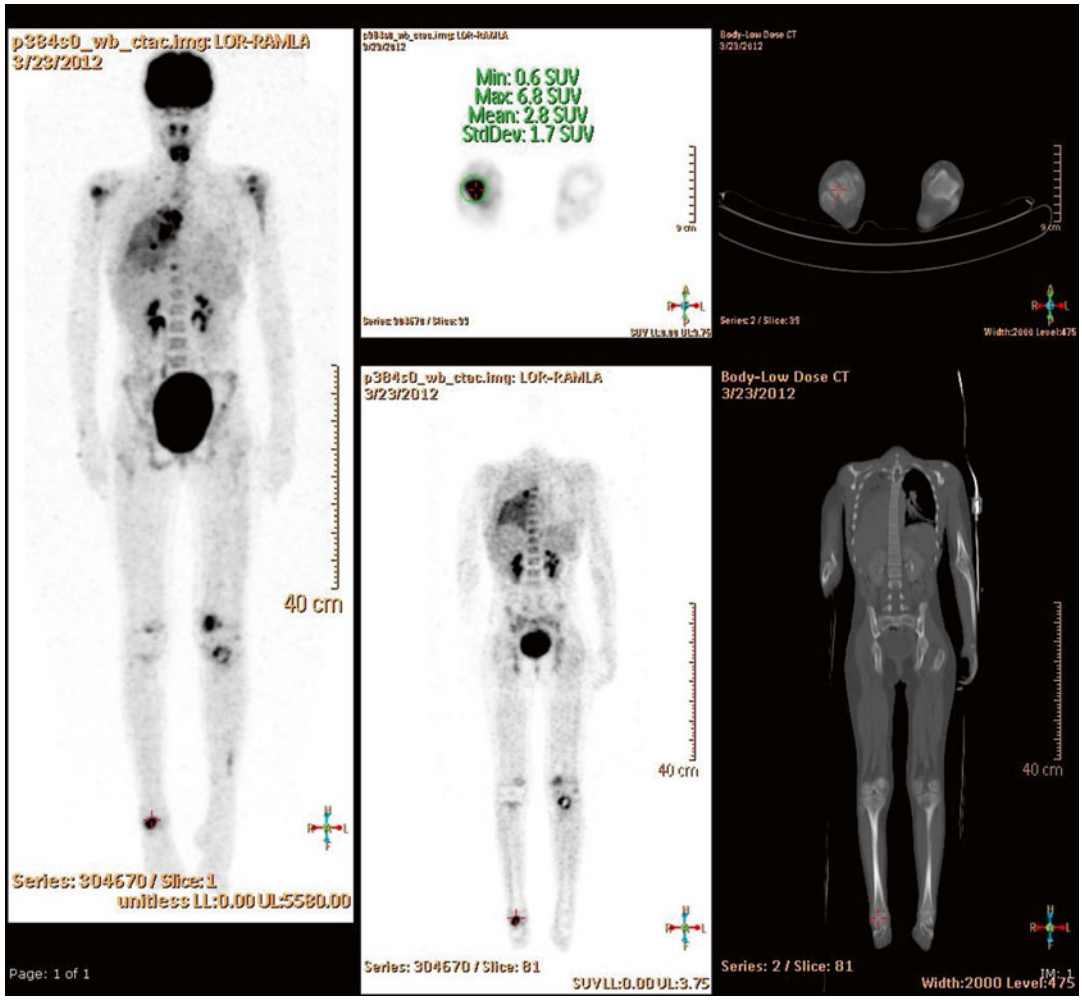

Fig. 14.27

adolescents or young adults. Advanced local disease and distant hematogenous metastases are typical. NMC is genetically defined by chromosomal rearrangements of the NUT gene on chromosome 15q14 forming a BRD4-NUT fusion oncogene which blocks epithelial differentiation, resulting in uncontrolled cell growth (Figs. 14.26 and 14.27).

Case 14.15: Recurrent Left Frontal Anaplastic Astrocytoma

Findings

Arrows point to a recurrent left frontal anaplastic astrocytoma (Fig. 14.28).

Discussion

High-grade gliomas (HGG)—glioblastoma multiforme (GBM), anaplastic astrocytoma, oligodendroglioma, and oligoastrocytoma—nearly always recur, with median overall survival (OS) ranging from 4 to 8 months from the time of progression (Fig. 14.28).

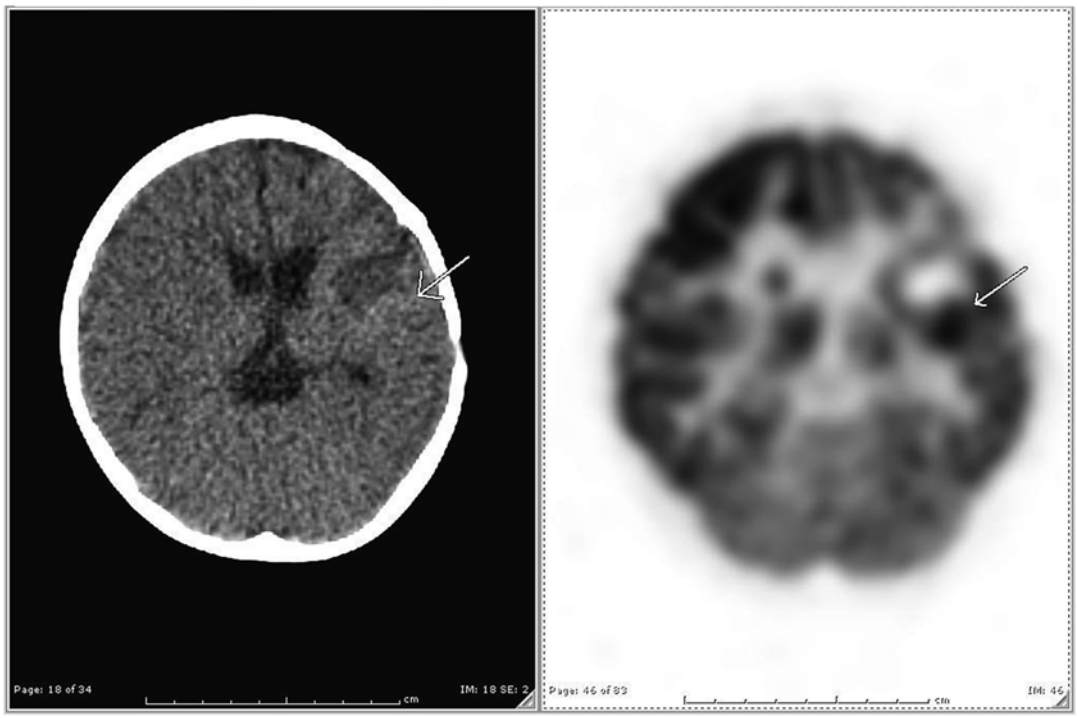

Fig. 14.28

Case 14.16: Ewing Sarcoma

Findings

There is increased uptake corresponding to the sclerotic lesion in the distal right tibia (Fig. 14.29).

Discussion

Ewing sarcoma family tumors account for approximately 3 % of all pediatric cancers, making them the second most common bone malignancies in children and adolescents. Radiologic evaluation of Ewing sarcoma can help detect and accurately assess the extent of disease prior to treatment, determine whether metastatic or recurrent disease is present, and monitor therapy response (Fig. 14.29).

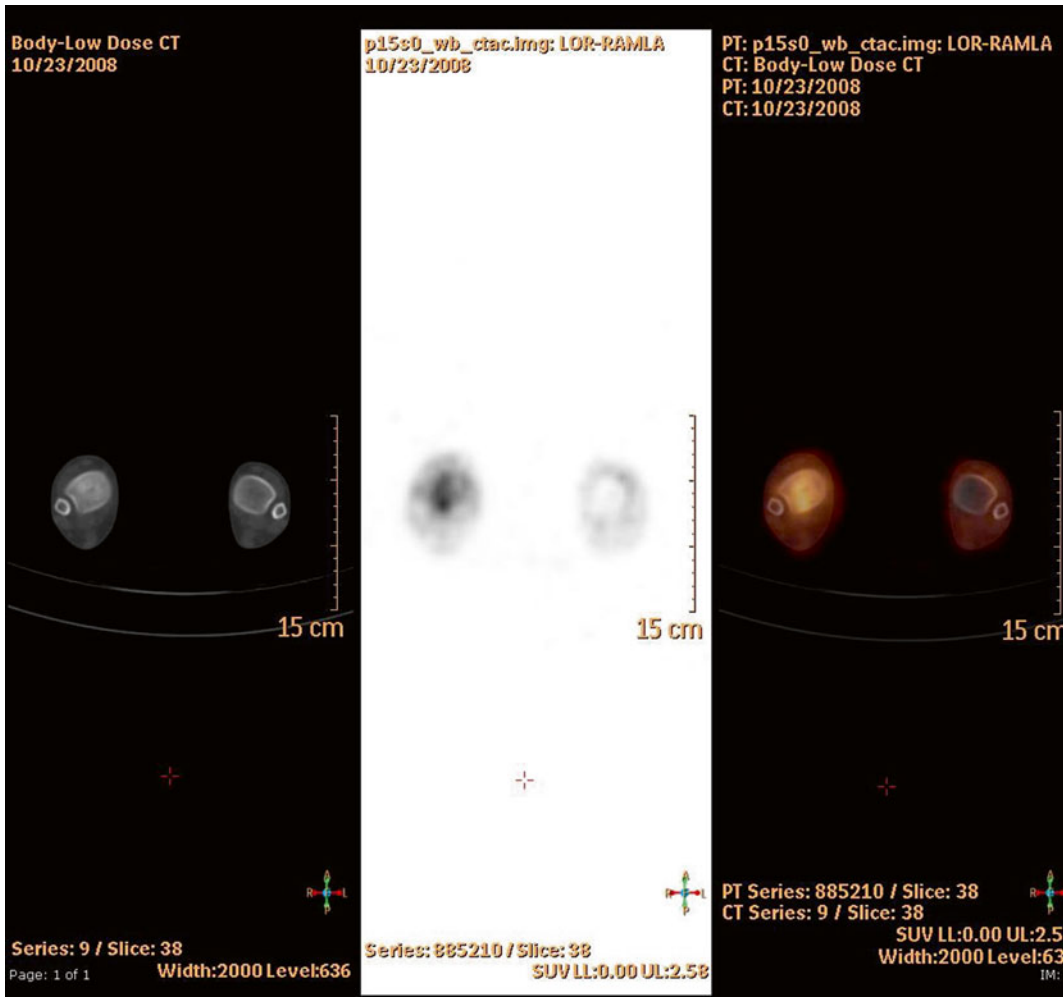

Fig. 14.29

Case 14.17: Posttransplant Lymphoproliferative Disorder

Findings

There is a soft tissue mass with FDG uptake in the right pelvis adjacent to the patient's transplanted kidney (Fig. 14.30).

Discussion

Posttransplant lymphoproliferative disease (PTLD) is a severe complication after solid organ or bone marrow transplantation. In pediatric transplant recipients, PTLD is the most common malignancy (Fig. 14.30).

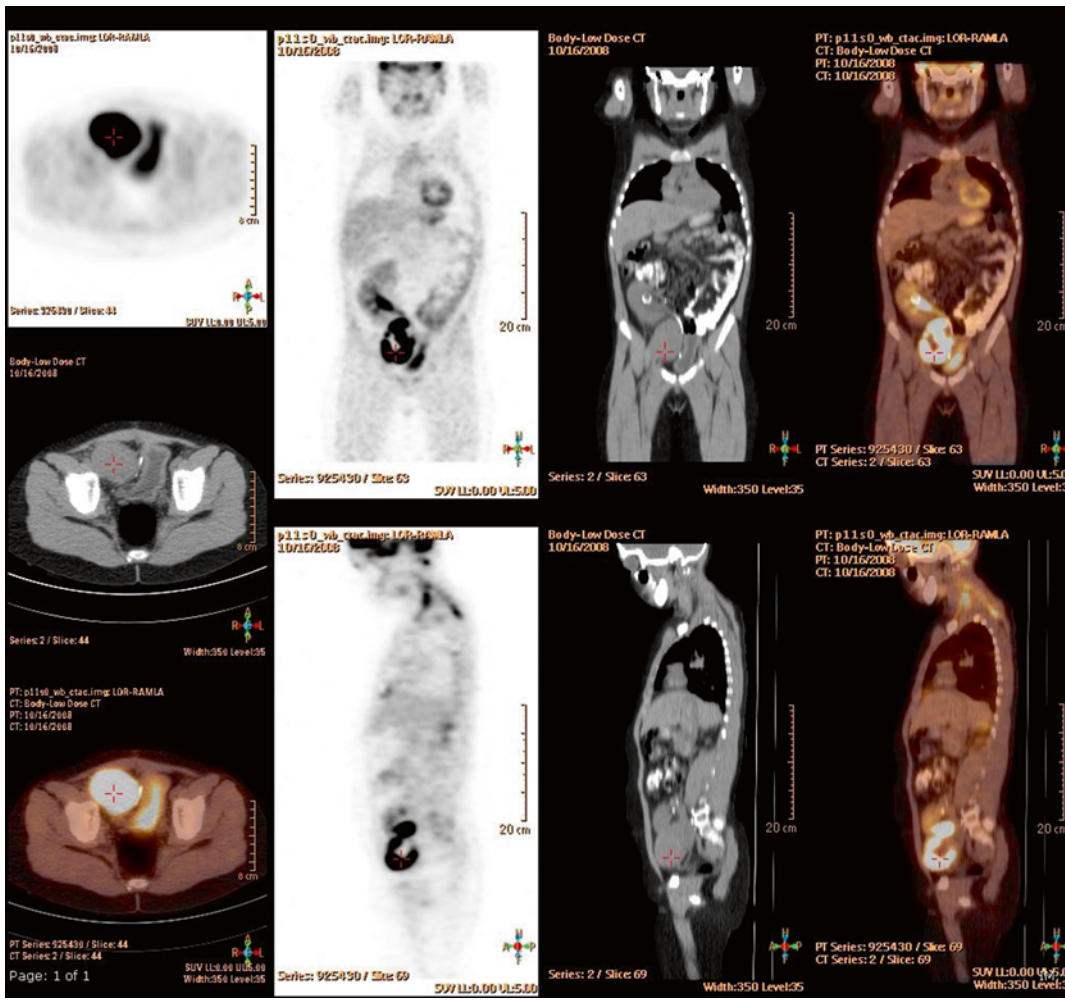

Fig. 14.30

Suggested Reading

1. Agrawal K, Mittal B, Harisankar C, Kuruva M, Bhattacharya A, Bansal D, Trehan A, Marwaha RK. Can F-18 FDG PET/CT avoid bone marrow biopsy in pediatric Hodgkin's lymphoma? India J Nucl Med. 2011;52 Suppl 1:399.
2. Aide N, Cappele O, Bottet P, Bensadoun H, Regeasse A, Comoz F, Sobrio F, Bouvard G, Agostini D. Efficiency of [(18)F] FDG PET in characterising renal cancer and detecting distant metastases: a comparison with CT. Eur J Nucl Med Mol Imaging. 2003;30(9):1236–45.
3. Ak I, Can C. F-18 FDG PET in detecting renal cell carcinoma. Acta Radiol. 2005;46(8):895–9.
4. Becherer A, Vierhapper H, Pötzi C, Karanikas G, Kurtaran A, Schmaljohann J, Staudenherz A, Dudczak R, Kletter K. FDG-PET in adrenocortical carcinoma. Cancer Biother Radiopharm. 2001;16(4):289–95.
5. Bestic JM, Peterson JJ, Bancroft LW. Use of FDG PET in staging, restaging, and assessment of therapy response in Ewing sarcoma. RadioGraphics. 2009;29:1487–500.
6. Brink I, Reinhardt MJ, Hoegerle S, Altehoefer C, Moser E, Nitzsche EU. Increased metabolic activity in the thymus gland studied with 18F-FDG PET: age dependency and frequency after chemotherapy. J Nucl Med. 2001;42(4):591–5.
7. Choi JY, Lee KS, Kim H-J, Shim YM, Kwon OJ, Park K, Baek C-H, Chung JH, Lee K-H, Kim B-T. Focal thyroid lesions incidentally identified by integrated ^{18}F-FDG PET/CT: clinical significance and improved characterization. J Nucl Med. 2006;4:609–15.
8. Clarke JR, Brglevska S, Lau EW, Ramdave S, Hicks RJ. Atypical brown fat distribution in young males demonstrated on PET/CT. Clin Nucl Med. 2007;32(9):679–82.
9. Coccia P, Ruggiero A, Rufini V, Maurizi P, Attiná G, Riccardo M, Natale L, Leccisotti L, Calcagni ML, Riccardi R. Cardiac metastases of Ewing sarcoma detected by 18F-FDG PET/CT. J Pediatr Hematol/Oncol. 2012;34(3):236–8.
10. Delbeke D, Martin W. Update of PET and PET/CT for hepatobiliary and pancreatic malignancies. HBP. 2005;7(3):166–79.
11. Freudenberg LS, Antoch G, Jentzen W, Pink R, Knust J, Görges R, Müller SP, Bockisch A, Debatin JF, Brandau W. Value of ^{124}I-PET/CT in staging of patients with differentiated thyroid cancer. Eur Radiol. 2004;14:2092–8.
12. Gawande RS, Khurana A, Messing S, Zhang D, Castañeda RT, Goldsby RE, Hawkins RA, Daldrup-Link HE. Differentiation of normal thymus from anterior mediastinal lymphoma and lymphoma recurrence at pediatric PET/CT. Radiology. 2012;262(2):613–22.
13. Groves AM, Win T, Screaton NJ, Berovic M, Endozo R, Booth H, Kayani I, Menezes LJ, Dickson JC, Ell PJ. Idiopathic pulmonary fibrosis and diffuse parenchymal lung disease: implications from initial experience with 18F-FDG PET/CT. J Nucl Med. 2009;50(4):538–45.
14. Hernandez-Pampaloni M, Takalkar A, Yu JQ, Zhuang H, Alavi A. F-18 FDG-PET imaging and correlation with CT in staging and follow-up of pediatric lymphomas. Pediatr Radiol. 2006;36(6):524–31.
15. Hudson MM, Krasin MJ, Kaste SC. PET imaging in pediatric Hodgkin's lymphoma. Pediatr Radiol. 2004;34(3):190–8.
16. Inoue K, Okada K, Taki Y, Goto R, Kinomura S, Fukuda H. (18)FDG uptake associated with CT density on PET/CT in lungs with and without chronic interstitial lung diseases. Ann Nucl Med. 2009;23(3):277–81.

17. Jadvar H, Fischman AJ. Evaluation of rare tumors with [F-18] Fluorodeoxyglucose positron emission tomography. Clin Positron Imaging. 1999;2(3):153–8.
18. Kabickova E, Sumerauer D, Cumlivska E, Drahokoupilova E, Nekolna M, Chanova M, Hladikova M, Kodet R, Belohlavek O. Comparison of ^{18}F-FDG-PET and standard procedures for the pretreatment staging of children and adolescents with Hodgkin's disease. Eur J Nucl Med Mol Imaging. 2006;33(9):1025–31.
19. Kaneta T, Hakamatsuka T, Yamada T, Takase K, Sato A, Higano S, Kinomura S, Fukuda H, Takahashi S, Yamada S. Case Report: FDG PET in solitary metastastic/secondary tumor of the kidney: a report of three cases and a review of the relevant literature. Ann Nucl Med. 2006;20(1):79–82.
20. London K, Cross S, Onikul E, Dalla-Poza L, Howman-Giles R. 18F-FDG PET/CT in paediatric lymphoma: comparison with conventional imaging. Eur J Nucl Med Mol Imaging. 2011;38(2):274–84.
21. Louis DN, Ohgaki H, Wiestler OD, et al. The 2007 WHO classification of tumours of the central nervous system. Acta Neuropathol. 2007;114:97–109.
22. Lucas JD, O'Doherty MJ, Wong JC, Bingham JB, McKee PH, Fletcher CD, Smith MA. Evaluation of fluorodeoxyglucose positron emission tomography in the management of soft-tissue sarcomas. J Bone Joint Surg Br. 1998; 80(3):441–7.
23. Ludwig JA. Ewing sarcoma: historical perspectives, current state-of-the-art, and opportunities for targeted therapy in the future. Curr Opin Oncol. 2008;20(4):412–8.
24. Mackie GC, Shulkin BL, Ribeiro RC, Worden FP, Gauger PG, Mody RJ, Connolly LP, Kunter G, Rodriguez-Galindo C, Wallis JW, Hurwitz CA, Schteingart DE. Use of [^{18}F]Fluorodeoxyglucose positron emission tomography in evaluating locally recurrent and metastatic adrenocortical carcinoma. J Clin Endocrine Metab. 2006;91:2665–71.
25. Makis W, Lisbona R, Derbekyan V. Hodgkin lymphoma post-transplant lymphoproliferative disorder following pediatric renal transplant: serial imaging with F-18 FDG PET/CT. Clin Nucl Med. 2010;35(9):704–5.
26. McCarville MB, Christie R, Daw NC, Spunt SL, Kaste SC. PET/CT in the evaluation of childhood sarcomas. Am J Roentgenol. 2005;184(4):1293–304.
27. Mirzaei S, Knoll P, Kohn H. Diagnosis of recurrent astrocytoma with fludeoxyglucose F18 PET scanning. NEJM. 2001;344:2030–1.
28. Niederkohr RD, Cameron MJ, French CA. FDG PET/CT imaging of NUT midline carcinoma. Clin Nucl Med. 2011;36(9):e124–6.
29. Nusair S, Rubinstein R, Freedman NM, Amir G, Bogot NR, Izhar U, Breuer R. Positron emission tomography in interstitial lung disease. Respirology. 2007;12(6):843–947.
30. Rhodes MM, Delbeke D, Whitlock JA, Martin W, Kuttesch JF, Frangoul HA, Shankar S. Utility of FDG-PET/CT in follow-Up of children treated for Hodgkin and Non-Hodgkin lymphoma. J Pediatr Hematol Oncol. 2006; 28(5):300–6.
31. Riad R, Omar W, Kotb M, Hafez M, Sidhom I, Zamzam M, Zaky I, Abdel-Dayem H. Role of PET/CT in malignant pediatric lymphoma. Eur J Nucl Med Mol Imaging. 2010;37(2):319–29.
32. Sahani DV, Kalva SP. Imaging the liver. The Oncologist. 2004;9(4):385–97.
33. Shammas A, Lim R, Charron M. Pediatric FDG PET/CT: physiologic uptake, normal variants, and benign conditions. RadioGraphics. 2009;29:1467–86.
34. Shammas A, Degirmenci B, Mountz JM, McCook BM, Branstetter B, Bencherif BB, Joyce JM, Carty SE, Kuffner HA, Avril N. ^{18}F-FDG PET/CT in patients with suspected recurrent or metastatic well-differentiated thyroid cancer. J Nucl Med. 2007;48(2):221–6.

35. Tateishi U, Hosono A, Makimoto A, Nakamoto Y, Kaneta T, Fukuda H, Murakama K, Terauchi T, Suga T, Inoue T. Comparative study of FDG PET/CT and conventional imaging in the staging of rhabdomyosarcoma. Ann Nucl Med. 2009;23(2):155–61.
36. von Falck C, Maecker B, Schirg E, Boerner AR, Knapp WH, Klein C, Galanski M. Post transplant lymphoproliferative disease in pediatric solid organ transplant patients: a possible role for [^{18}F]-FDG-PET(/CT) in initial staging and therapy monitoring. Eur J Radiol. 2007;63:427–35.
37. Wang K-B, Tsai S-C, Chen Y-C. A possible musculoskeletal pitfall in 18F-FDG PET: nodular fascitis. Ann Nucl Med Sci. 2010;23:165–8.
38. Yun M, Kim W, Alnafisi N, Lacorte L, Jang S, Alavi A. ^{18}F-FDG PET in characterizing adrenal lesions detected on CT or MRI. J Nucl Med. 2001; 42(12):1795–9.